

**Performance analysis of CH₃NH₃PbI₃ Perovskite based Solar Cell with All-Metal-
Oxide Transport Layers**

BY

MAHAMUDUL HASAN PRIO

ID NO: 181-31-252

**This Report Presented in Partial Fulfillment of the Requirements for the
Degree of Master of Science in Electronics and Telecommunication
Engineering**

Supervised By

Md. Taslim Arefin

Associate Professor

Department of ETE

Daffodil International University



DAFFODIL INTERNATIONAL UNIVERSITY

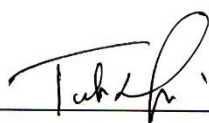
DHAKA, BANGLADESH

SEPTEMBER 2019

APPROVAL

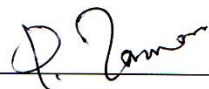
This Project titled “**Simulation based study of CH₃NH₃PbI₃**”, submitted by Hasib Rahman to the Department of Electronics and Telecommunication Engineering, Daffodil International University, has been accepted as satisfactory for the partial fulfillment of the requirements for the degree of M.Sc. in Electronics and Telecommunication Engineering and approved as to its style and contents. The presentation was held on 27 October, 2019.

BOARD OF EXAMINERS



(Md. Taslim Arefin)
Associate Professor & Head
Department of ETE
Faculty of Engineering
Daffodil International University

Chairman



(Dr. M. Quamruzzaman)
Professor
Department of ETE
Faculty of Engineering
Daffodil International University

Internal Examiner



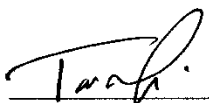
(Dr. Md. Fayzur Rahman)
Professor & Chairperson
Department of EEE
Green University

External Examiner

DECLARATION

I hereby declare that, this project has been done by us under the supervision of **Md. Taslim arefin**, Associate professor, Department of ETE Daffodil International University. I have also declare that neither this project nor any part of this project has been submitted elsewhere for award of any degree or diploma.

Supervised by:



Md. Taslim Arefin
Associate professor
Department of ETE
Daffodil International University

Submitted by:
mahamudul hasan prio

Mahamudul hasan prio
ID: 181-31-252
Department of ETE
Daffodil International University

ACKNOWLEDGEMENT

First we express our heartiest thanks and gratefulness to almighty Allah for His divine blessing makes us possible to complete this project successfully.

I fell grateful to and wish my profound our indebtedness to Supervisor Md. Taslim Arefin, Associate professor Department of ETE Daffodil International University, Dhaka. Deep Knowledge & keen interest of my supervisor in the field of power section influenced me to carry out this thesis. His endless patience ,scholarly guidance ,continual encouragement , constant and energetic supervision, constructive criticism , valuable advice, reading many inferior draft and correcting them at all stage have made it possible to complete this project.

I would like to express my heartiest gratitude to parents, friends, classmates and Head, Department of ETE, for his kind help to finish my thesis and also to other faculty member and the staff of ETE department of Daffodil International University.

Finally, I must acknowledge with due respect the constant support and patients of our parents.

Abstract

Due to cheap and simple solution processed fabrication feasibility, excellent electrical and optical properties as well as thinness, semi-transparency and flexibility, organic inorganic perovskites like $\text{CH}_3\text{NH}_3\text{PbI}_3$ (MAPbI_3) have recently been unfolded as one of the most promising contender of third generation solar cells. Starting in 2009 with only 3% power conversion efficiency (PCE), perovskite solar cells have achieved over 22% PCE in the recent times thanks to rigorous research interest both in academic and industry level.

To avail flexible configurations, perovskite solar cell structure has been evolved from mesoscopic to planar because of flexible substrates lower transition temperature. Furthermore, due to low cost fabrication, higher mobility and above all, proper band alignment, transparent / high bandgap metal oxides have been studied of late to replace conventionally used electron transport materials (ETM) like TiO_2 and hole transport materials (HTM) like organic Spiro OMeTAD or PEDOT:PSS.

In this work, MAPbI_3 perovskite solar cell (inverted planar structure) is studied in details for all-metal-oxide transport layers using SCAPS 1D simulation software. ZnO and SnO_2 along with TiO_2 are chosen as ETMs for cells with NiO_x and Cu_2O as HTMs owing to their better band alignment, higher mobility and carrier concentration. The study mainly focused on the comparative performance of these three ETMs. Variation of perovskite layer thickness, perovskite bulk defect density and perovskite-ETM interface states are included thoroughly for this contrasting simulation based study. It is found that these metal oxides can be considered potential and for some cases, better contender as transport layers for planar perovskite solar cells to move towards flexible configurations.

Table of contents

DECLARATION	II
CERTIFICATION	III
DEDICATION	IV
ACKNOWLEDGEMENTS	V
ABSTRACT	VI
LIST OF TABLES	X
LIST OF FIGURES	XI

List of Contents:

Chapter 1

Introduction	1
1.1 Renewable Energy	1
1.2 Objective	2
1.3 Thesis outline	3

Chapter 2

Perovskite Solar Cell	4
2.1 Perovskite	4
2.2 Structure of Perovskite	5
2.3 Application of Perovskite	5
2.3.1 Photovoltaic Operation (Solar Cell)	5
2.3.2 Light Emitting Diode	5
2.3.3 Other application	6
2.4 Perovskite as Solar Cell	7
2.4.1 Structure	7
2.4.2 History of Perovskite Solar Cell	8
2.4.3 Properties of Perovskite Solar Cell	9

2.4.4 Operation	9
2.4.5 Advantages	10
2.4.6 Disadvantages	11
2.4.7 Progress over the year	13
2.5 Electron Transport Layer (ETL)	15
2.6 Common Material	16
2.7 Properties of a good ETL	16
Chapter 3	
Simulation of MAPbI₃ Perovskite Solar Cell for All Oxide Transport Layers: Methodology	17
3.1 Solar Cell Structure	17
3.2 SCAPS Input	18
3.2.1 Parameter Selection of Various Layers	18
3.2.2 Absorption Model	19
3.2.3 Contact	21
3.2.4 Illumination	21
3.2.5 Bulk Defect and Interface State	21
3.2.6 Selection of defect and interface Parameters	23
3.3 Simulation for Different Structure containing All-Metal-Oxide Transport Layers	24
Chapter 4	
Result and Discussion	26
4.1 Analysis with Fixed Properties	26
4.2 Analysis Varying Perovskite Thickness	29
4.3 Analysis Varying Perovskite Bulk Defect Density	31
4.4 Analysis Varying Perovskite-ETM Interface Defect Density	34
Chapter 5	
Conclusion	39
5.1 Limitation	40
5.2 Future work	40
Appendix-1	

Data Table from Simulation	41
References	66

LIST OF TABLES

Table No	Table name	Pageno.
Table 2.1	Perovskite- phase Metal Oxide: Properties and Application	06
Table 3.1	Properties of different layer used in SCAPS simulation	18
Table 3.2	Shows the defect levels used in our simulation	23
Table 4.1	Performance parameters of different perovskite solar cell structures.	28
Table 4.2	Thickness for maximum efficiency	30

LIST OF FIGURES

Figure No	Name	Page
Fig. 2.1	Perovskite mineral (CaTiO_3).	4
Fig. 2.2	Crystal structure belonging to perovskite structure	5
Fig. 2.3	Perovskite solar cells (a) typical structure (b) Practical structure.	7
Fig. 2.4	Crystal structure of $\text{CH}_3\text{NH}_3\text{PbI}_3$ perovskite where organic cation CH_3NH_3^+ , metal cation Pb^{2+} , and halide anion I^-	8
Fig. 2.5	Gradually improvement in perovskite solar cell device	9
Fig. 2.6	Band diagram and main processes and perovskite solar cell: 1 Absorption of photon and free charge generations; 2 charge Transport; 3 Charge extraction	10
Fig. 2.7	Stability of perovskite material	11
Fig. 2.8	Hysteresis curve of perovskite solar cell	12
Fig. 2.9	Perovskite solar cells have increased in power conversion efficiency at a phenomenal rate compared to other type photovoltaics. Although this figure only represents lab - based “hero cells “, it heralds great promise	12
Fig. 2.10	Year by year perovskite solar cell patents	13
Fig. 2.11	Perovskite solar cell efficiencies over the year	14
Fig.3.1	Simulated Structure of Perovskite Solar Cell	17
Fig.3.2	SCAPS different properties of each layer	18
Fig.3.3	Absorption Curve used in simulation for different layer	20

Fig.3.4	Solar-spectrum-of-AM 1.5 G	21
Fig.3.5	Sample window of SCAPS for defect input (a) Bulk defect (b) Interface defect.	22
Fig.3.6	Comparison between Experimental (fabrication) result from Tze-Bin song et. al (2015) and our simulated work using SCAPS. The table shows the numerical values.	24
Fig.3.7	Flowchart of complete method of our work	25
Fig.4.1	I-V characteristics of Cu ₂ O-MAPbI ₃ structure for different ETMs.	27
Fig.4.2	I-V characteristics of NiO _x -MAPbI ₃ structure for different ETMs.	28
Fig.4.3	Performance of perovskite solar cell for different perovskite thickness	29
Fig.4.4	Performance of perovskite solar cell for different perovskite defect density.	31
Fig.4.5	Band alignment of different materials used in simulation	32
Fig.4.6	Analysis of Perovskite Solar Cell for Different Perovskite ETL interface State at Bulk Defect 10^{15}cm^{-3}	34
Fig.4.7	Effect of ETL-Perovskite Interface and Perovskite bulk defect on Efficiency for different Structure	37

Chapter 1

Introduction

Renewable energy is any energy source that is naturally replenished, like that derived from solar, wind, geothermal or hydroelectric action. Energy produced from the refining of biomass is also often classified as renewable. Coal, oil or natural gas, on the other hand, are finite sources [1].

The most common definition is that renewable energy is from an energy resource that is replaced rapidly by a natural process such as power generated from the sun or from the wind. Most renewable forms of energy, other than geothermal and tidal power, ultimately come from the Sun.

Renewable Energy uses energy resources and technologies that are “clean” or “green” because they produce few if any pollutants. Many people use the terms “Alternative Energy”, “Renewable Energy” and even “Green Energy” [2].

Solar energy is a renewable free source of energy it's convert of energy from sunlight into electricity. Solar panel efficiency of conversion rate refers to how much of the incoming solar energy is converted into electrical power. The most efficiency solar panels on the market today have efficiency rating as high as 22.8%, but most using 15% to 17% efficiency. Solar panels used by military, space exploration agencies and in tight tolerance critical applications have significantly higher efficiency however they are also very expensive. This literature deals with commercial solar panels that are affordable by general populace.

1.1 Types of Solar Cell:

There are three major cell types that classified by its manufacturing technology and the semiconductor.

- Crystalline silicon PV module.
- Amorphous silicon PV module.

- Hybrid silicon PV module

Another types of solar cell

- Thin film solar cell
- Copper indium gallium selenide solar cells.
- Multi junction solar cell.
- Organic solar cell.
- Photo Electro chemical solar cell.
- Polymer solar cell.

1.2 Objective:

The aim and objective of this thesis work is to

- Study $\text{CH}_3\text{NH}_3\text{PbI}_3$ perovskite solar cell with all metal oxide transport layer
- Perform simulation in SCAPS software package to study the proposed solar cell structure using Cu_2O & NiO_x (separate simulations) as hole transport layer (HTL) and TiO_2 , SnO_2 , & ZnO as electron transport layer (ETL)
- Take reading of open circuit voltage, short circuit current, fill factor and efficiency for each aforementioned material for a comparative study
- Observe the variation of these respective structure for different thickness and defect density of perovskite layer

1.3 Thesis Outline:

This thesis paper constitutes of 5 chapter including the solar cell. This chapter includes explains the simulation based study of methane ammonium lead iodate ($\text{CH}_3\text{NH}_3\text{PbI}_3$).

Chapter: 1 Explain and general introduction related to the objective of this thesis .

Chapter: 2 In this chapter, we summarize the perovskite material, structure of perovskite and also discuss operation principle of perovskite solar cell, application, properties and electron transport material.

Chapter: 3 Simulation of MAPbI_3 Perovskite Solar Cell for All Oxide Transport Layers: Methodology.

Chapter: 4 These Based on the methodology described in chapter 3 simulations are performed for six inverted planar perovskite structures.structures.

Chapter: 5 gives conclusion about this thesis and the future work suggestions.

Chapter 2

Perovskite Solar Cell

In this article, we summarize the perovskite material, structure of perovskite and also discuss operation principle of perovskite solar cell, application, properties and electron transport material.

2.1 Perovskite:

A perovskite is any material with the same type of crystal structure as calcium titanium oxide (CaTiO_3) known as the perovskite structure $^{\text{XII}}\text{A}^{2+}\text{VI}\text{B}^{4+}\text{X}^{2-}_3$. Simultaneously the general chemical formula for perovskite compounds in ABX_3 where A and B are two cations and X is an anion. It is named after Russian mineralogist Lev perovskite.



Fig: 2.1 Perovskite mineral (CaTiO_3).

2.2 Structure of Perovskite:

Basic structure of perovskite is shown below –

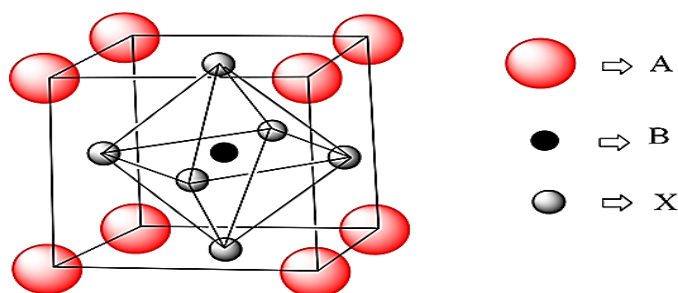


Fig: 2.2 Crystal structure belonging to perovskite structure.

2.3 Application of Perovskite:

Perovskite has multiple applications in the silicon technology manufacturing industry.

Some of them are discussed as follows.

2.3.1 Photovoltaic Operation (Solar Cell):

In Solar Cell, a few years ago photovoltaics have been expensive because of the high price of the raw materials and the complex fabrication methods. Now with the development of perovskites we are working towards a cheaper and more efficient solar cells. The efficiency has risen to a confirmed efficiency of 17.9% and it can be done in one year ahead of 21% will increase. This will be discussed further in the next part.

2.3.2 Light Emitting Diode:

As LED (Light Emitting Diode), metal halide perovskite is emerging as one of the most promising materials for light emitting diode due to it being easy to prepare, having a low cost, and having a high performance. One important advantage of perovskite in LED application is that they usually have high color purity with the full width half maximum of ~ 15-25nm for the electroluminescence spectra. Another advantages are the color tenability over the whole visible spectrum by simply changing the content of different halides within the compounds.

2.3.3 Other Applications:

The properties applications of a number of important perovskite phase mixed-metal oxides are summarized in Table 2.1. The uses for these material are based upon their intrinsic dielectric, ferroelectric, piezoelectric and pyroelectric properties of relevance in

corresponding electronics application such as electromechanical devices, transducers, capacitors, actuators, dynamic random access memory, field effect transistors and logic circuitry.

Table:2.1 Perovskite-phase Metal Oxide: Properties and Application.

Materials	Properties	Application
BaTiO ₃	Dielectric	capacitor, sensor
(Ba,Sr)TiO ₃	Pyroelectric	Pyro detector
PbTiO ₃	Pyroelectric Piezoelectric	Pyro detector acoustic transducer
Pb(Zr,Ti)O ₃	Dielectric pyroelectric piezoelectric electro-optic	nonvolatile memory, pyro detector surface acoustic wave device, substrate waveguide device
(Pb,La)(Zr,Ti)O ₃	Pyroelectric electro-optic	Pyro detector waveguide device, optical memory display
LiNbO ₃	Piezoelectric	pyro detector, surface acoustic wave device
(LiNbO ₃ /Ti)	electro-optic	waveguide device, second harmonic generation, optical modulator
K(Ta,Nb)O ₃	Pyroelectric electro-optic	Pyro detector waveguide device, frequency doubler

2.4 Perovskite as Solar Cell:

2.4.1 Structure:

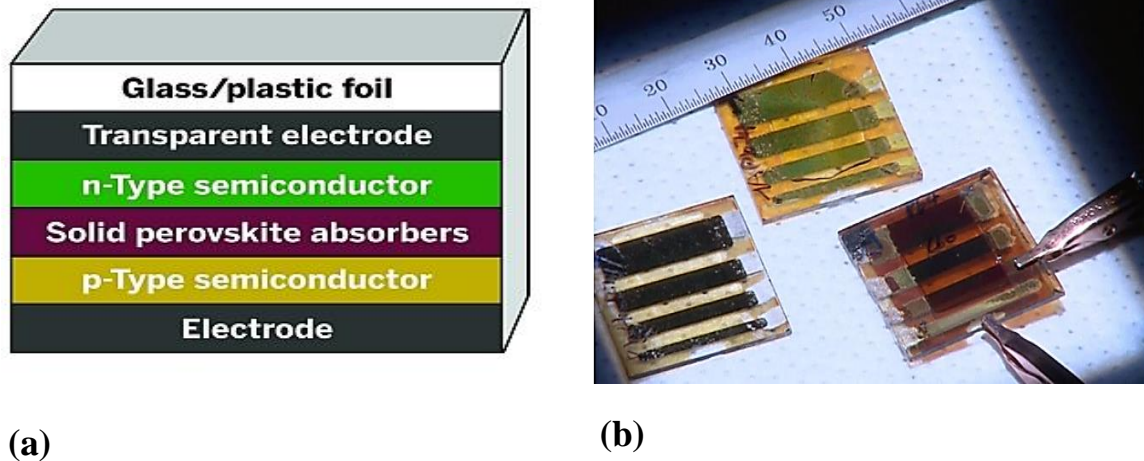


Fig: 2.3 Perovskite solar cells (a) typical structure (b) Practical structure

In this type of solar cells, perovskite material, such as lead halide perovskite $\text{CH}_3\text{NH}_3\text{PbI}_3$, act as photo absorbers to generates free carriers that can be collected in the electrodes through both p- and n- type semiconductor layers.

Also shown crystal structure of $\text{CH}_3\text{NH}_3\text{PbI}_3$ perovskite –

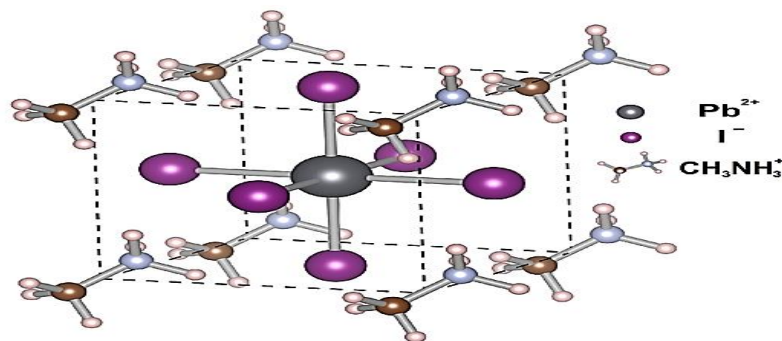


Fig: 2.4 Crystal structure of $\text{CH}_3\text{NH}_3\text{PbI}_3$ perovskite where organic cation CH_3NH_3^+ , metal cation Pb^{2+} , and halide anion I^-

2.4.2 History of Perovskite Solar Cell:

Miyasaka et al. in 2009 was developed the first perovskite solar cells. This was conventional dye sensitized solar cells. The structure of device was TiCl_4 treated fluorine-

doped tin oxide (FTO) (anode) / mesoporous TiO₂ /perovskite sensitizer /platinum coated FTO (cathode) and gap between the electrodes was filled with liquid electrolyte. With this structure, power conversion efficiencies (PCEs) of devices using MAPbBr₃ and MAPbI₃ were 3.13% and 3.81% respectively. Next research by Park et al. (2011) used initial liquid junction device and improved PCE 6.5% but the stability of the device could not be guaranteed. This was solved by using a solid state hole conductor spiro-OMeTAD on the top of perovskite layer instead of using liquid electrolyte this showed that long term stability for over 500 hole and PCE greater than 9%. Gratzel et al. used sequential deposition method in which PbI₂ was first deposited on mesoporous metal oxide and increase PCE almost 15%. Seok et al. (2014) PCE almost 16.2% by depositing uniform and dense perovskite layer. In 2015 Seok et al. achieved PCE greater than 20% by set up intermolecular exchange process. The conventional n-i-p structure in which electron extraction layer is deposited on bottom cathode and hole extraction layer under down the top anode layer and p-i-n structure which is the inverse of n-i-p type.

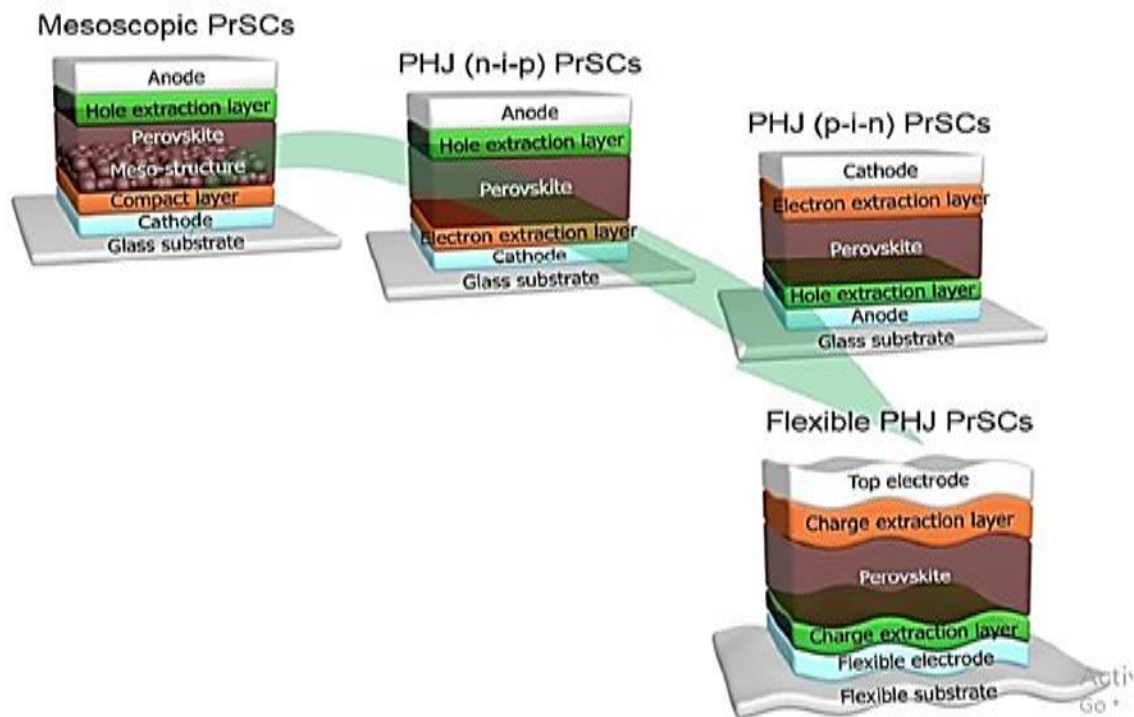


Fig:2.5 Gradual improvement in perovskite solar cell device.

2.4.3 Properties of Perovskite Solar Cell:

The distinct properties of perovskites are as follow as high absorption coefficients, tunable band gap, high charge carrier motilities, longer carrier diffusion length, allowing the photo-generated electrons and holes to travels long distance without energy loss as a result, the electrons and holes can travel through thicker solar cells, which absorbs more light and therefore generate more electricity than thin ones and the rapid increase in efficiency makes it a very interesting technology.

2.4.4 Operation:

A typical perovskite solar cell consists of an absorber layer, charge transporting layers and electrodes. The absorber layer which is composed of p-type and n-type material blend, serves as light harvester and at the same time ensures charge separation. The most widely used material for absorber layer in perovskite solar cell is the methyl ammonium lead iodide perovskite (which material we have used for this thesis work) which is placed between electron transporting layer and hole transporting layer was shown in figure.

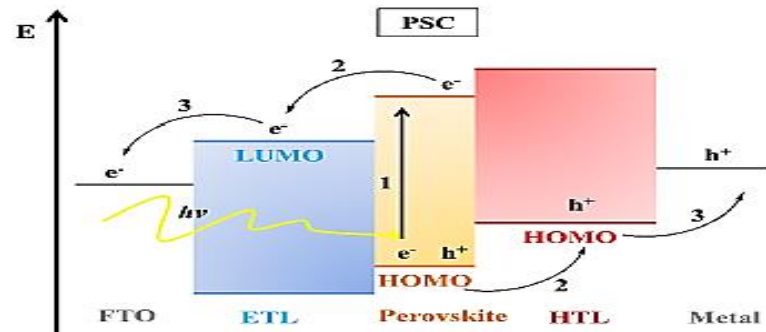


Fig:2.6 Band diagram and main processes and perovskite solar cell: 1 Absorption of photon and free charge generations; 2 charge Transport; 3 Charge extraction [13]

The valance and conduction band of the methyl ammonium lead iodide (MAPbI_3) are formed exclusively from Pb and I orbitals. The methyl ammonium cation does not participate electronically in the band structure, but controls the formation of the 3D perovskite crystal and therefore influence the optical properties of the material. In perovskite solar cells the light is absorbed by an absorber layer then a molecule absorbs light an electron is excited from the highest occupied molecular orbital (HOMO) to the lowest unoccupied molecular orbital (LUMO) in figure. An exciton is formed in absorber layer. Numerous studies reported a small exciton binding energy for perovskite absorber in

the range of a few milli-electron volts which indicates that practically the photon absorption leads to free-carrier generation. This non-excitonic nature of the charge generation is crucial for the development of high performance devices. In perovskite solar cells charge separation can occur either by injection of photo generated electrons into electron transport layer or injection of holes in hole transport layer. free electrons created near the perovskite /HTL interface have to diffuse through the entire width of the absorber layer before being extracted at the ETL/perovskite interface, with increased chances of recombination. Similar consideration apply to the holes near the ETL/perovskite interface. Recent reports demonstrated that both events electron injection and hole injection in the respective transporting layers occur in similar timescale.

2.4.5 Advantages:

Due to the improvement in the short time of perovskite solar cell, a lot of reasons some of them were discussed-

1. Efficiency:

The efficiency of the mineral has risen above 20% today. In the start of 2009, its efficiency was at 3%. Just a couple of years, perovskite solar cells have managed to achieve power conversion efficiency greater than or equal to that photovoltaics that have been around for nearly 40 years. That is why people are so excited about this mineral.

2. Cheaper:

Perovskite is also cheaper to produce than silicon. Researchers studying and developing the mineral believe that it may one day lead to solar panels that cost just 10 to 20 cents per watt. As of now, solar panels typically cost 75 cents per watt.

3. Absorption:

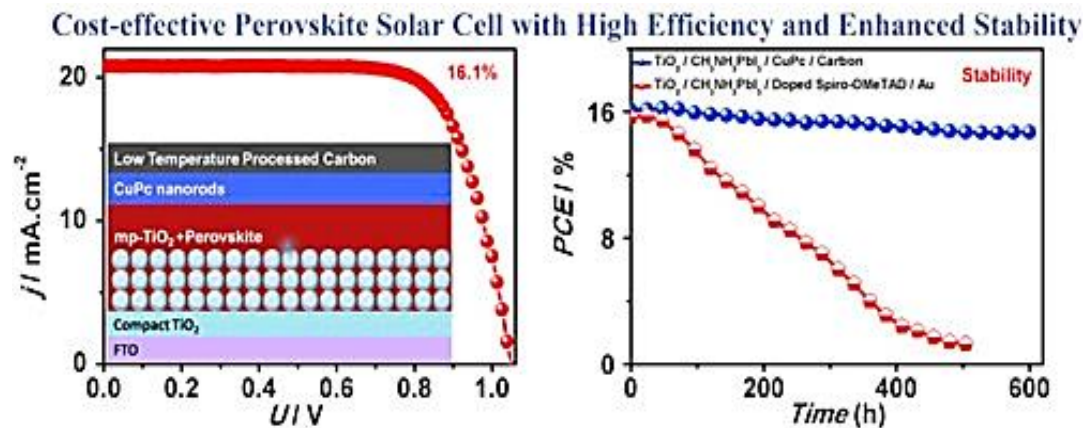
Perovskite is also very efficient in absorbing light. Recent study has found the mineral also emits light. It uses less material compared to silicon to absorb same amount light which result in cheaper solar power.

4. Cost:

The raw material used and the fabrication methods are both low cost. Their high absorption coefficient enables ultrathin films of around 500 nm to absorb the complete visible solar spectrum. These features combined result in the possibility to create low cost, high efficiency, thin, lightweight and flexible solar modules.

2.4.6 Disadvantages:

Despite the advantages, there are some problem it is discussed below-



1. Stability issues:

Perovskite breaks down fairly quick when exposed to heat, snow, moisture etc. One of the main disadvantages of perovskite material is its performance degradation with time. Infigure 2.7 we can see that.

Fig: 2.7 Stability of perovskite material.

With the increase in time, the stability decreases. To compensate this effect various improved structure are proposed by various research. One example is shown in above figure where performance is more stable.

2. Toxicity:

Methyl ammonium lead iodide is most widely used as perovskite material in absorber layer of perovskite solar cells. But lead (Pb) toxic for environment that's why Pb-free perovskite materials are on research.

3. Hysteresis:

High Performance perovskite solar cells based on organ metal halide perovskite have emerged in the past five years as excellent devices for harvesting solar energy.

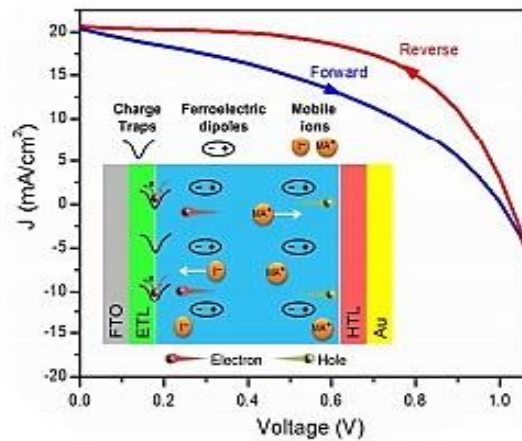


Fig: 2.8 Hysteresis curve of perovskite solar cell.

Some remaining challenges should be resolved to continue the momentum in their development. The photocurrent density-voltage (J-V) responses of the perovskite solar cells demonstrate anomalous dependence on the voltage scan direction/rate/range, voltage conditioning history and device configuration. The hysteresis J-V behavior presents a challenge for determining the accurate power conversion efficiency of the perovskite solar cells.

2.4.7 Progress over the year:

The improvement of the perovskite solar cell can be understood in the following graphs-

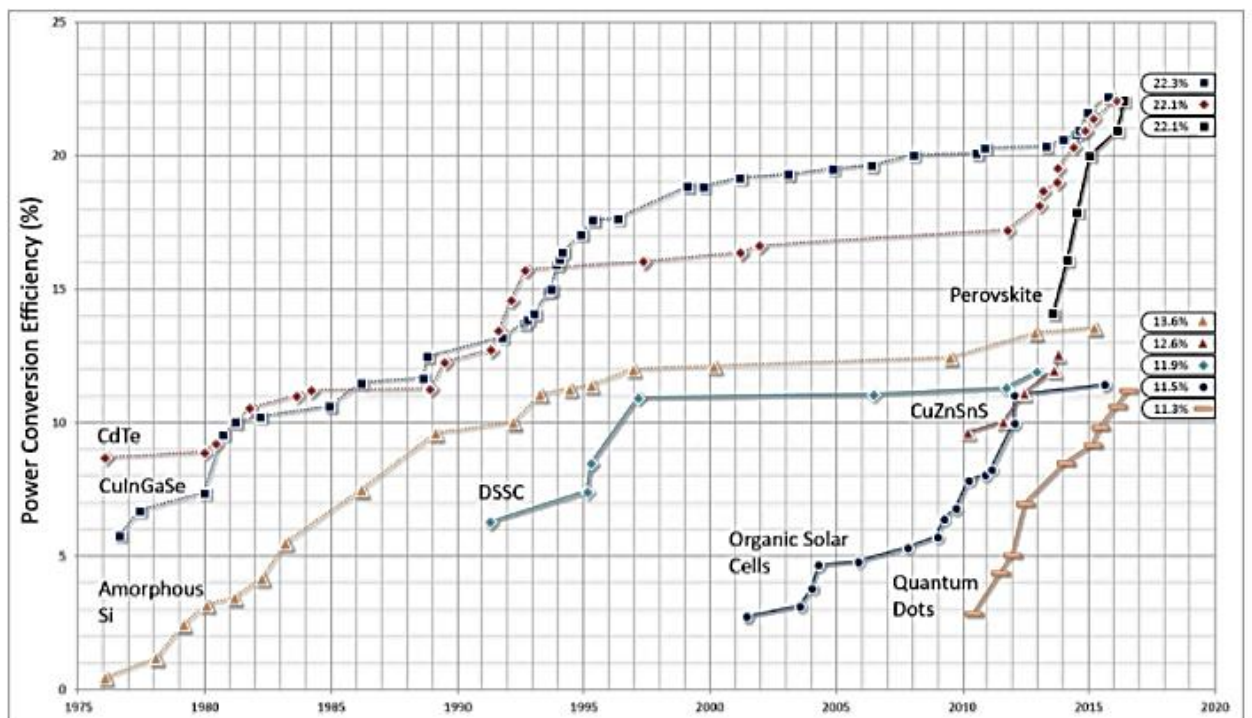
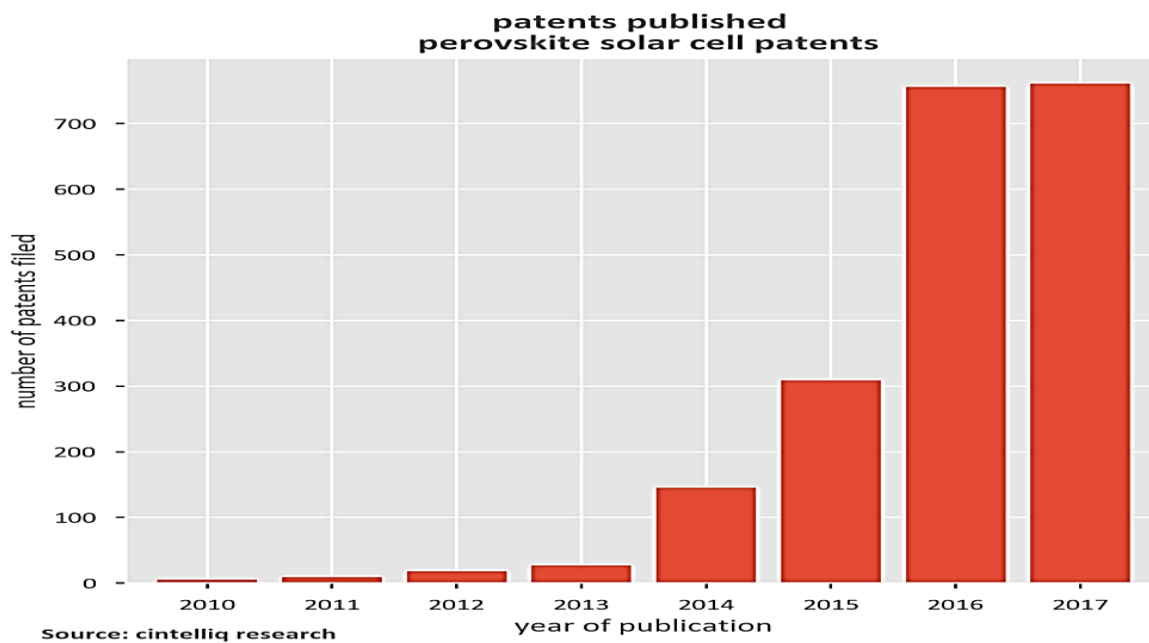


Fig:2.9 Perovskite solar cells have increased in power conversion efficiency at a phenomenal rate compared to other type photovoltaics. Although this figure only represents lab-based “hero cells”, it heralds great promise.

The figure 2.9 demonstrates the power conversion efficiencies of the perovskite based devices over recent year, in comparison to photovoltaic research technology. In the space of three years, perovskite solar cells have managed to achieve power conversion efficiencies compared to Cadmium Telluride, which has been around for nearly 40 years.

The dramatic rise in perovskite solar cell efficiency is still incredibly significant and impressive short period of time

Figure: 2.10 Year by year perovskite solar cell patents.



The latest perovskite patent landscape report from finds explosive growth in perovskite photovoltaic patent publications over the past two year. In 2016 and 2017 more than 1500 patents have been published representing 75% of all perovskite photovoltaic patents published since 2008. Not only is technical progress rapid but so too has been the transitions to commercial production.

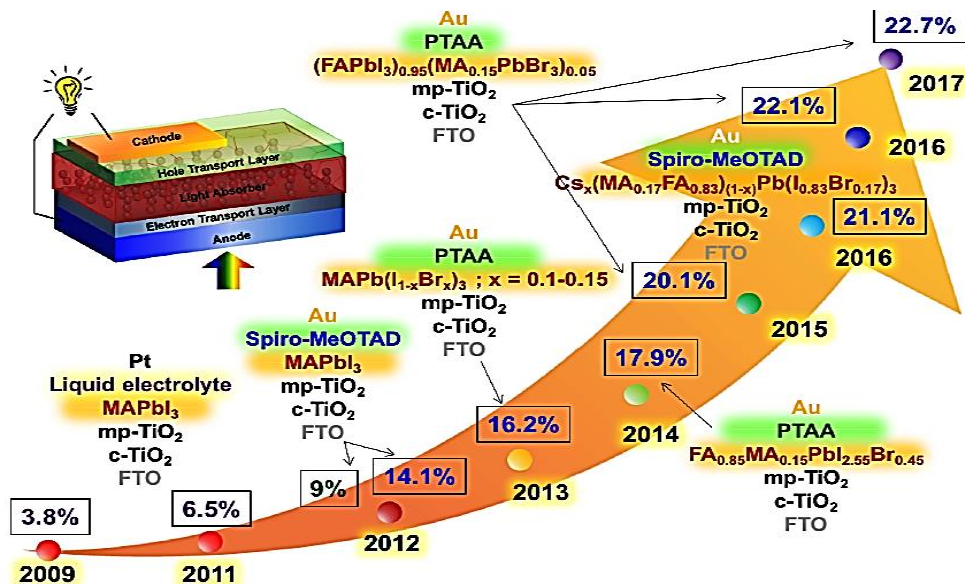


Fig:2.11 Perovskite solar cell efficiencies over the year.

Owing to intensive research efforts across the world since 2009, perovskite solar cell power conversion efficiencies are now comparable or even better than several other photovoltaic technologies.

2.5 Electron Transport Layer (ETL):

The electron transport layer is a layer which has a high electron affinity and high electron mobility. These characteristics allow electrons to follow across the layer.

2.6 Common Material:

The efficiency and stability of perovskite solar cells also depend strongly what type of materials selected as the electron transport layer in the device. So several different materials have been used for this task, in order to optimize both the performance and the stability-

Metal oxide-

Metal sulfides -

Non-ETLs-

Stannic oxide (TiO₂),

Zinc sulfide (ZnS),

Alumina (Al₂O₃),

Zinc oxide (ZnO),

Cadmium sulfide (CdS),

Zirconia (ZrO₂),

Stannic oxide (SnO₂),

Indium sulfide (In₂S₃)

Silica (SiO₂) etc.

Tungsten trioxide (WO₃),

Indium (III) oxide (In₂O₃),

Niobium pentoxide (Nb_2O_5),

Iron (III) oxide (Fe_2O_3),

Cerium oxide (CeO) etc.

2.7 Properties of a good ETL:

Electron transport layer enhance the electron extraction when employed as interfacial layers. When a molecule absorbs light an electron is excited from the highest occupied molecular orbital (HOMO) to the lowest unoccupied molecular orbital (LUMO) then it should higher than the perovskite absorber layer. So that a photon can pass through easily and be absorbed by the perovskite absorber for this reason it must have high transmittance in the ultraviolet to visible region. Extraction generation must be dissociated before collection either by electron transport layer or hole transport layer.

Chapter 3

Modeling and Simulation of MAPbI₃ Perovskite Solar Cell for All Oxide Transport Layers: Methodology

Due to lower fabrication cost, higher mobility and higher transmission of sun light oxide based hole and electron transport material(ETM) are gaining popularity over mostly used organic HTM like Spiro-OMeTAD and organic ETMs. In our work we have presented a simulation based study of MAPBI₃ Perovskite solar cell(PrSC) with oxide based HTMs like NiO_x and Cu₂O and ETMs like TiO₂, ZnO, and SnO₂. For our simulation we have used SCAPS (Version: 3.3.06) software which is a SCAPS [35] (a Solar Cell Capacitance Simulator) which is a one dimensional solar cell simulation program developed at the Department of Electronics and Information Systems (ELIS) of the University of Gent, Belgium.

In this chapter we have presented the methodology of our work along with the working procedures of SCAPS software.

3.1 Solar Cell Structure:

All simulation was done considering basic PrSC structure bas shown in figure. 3.1

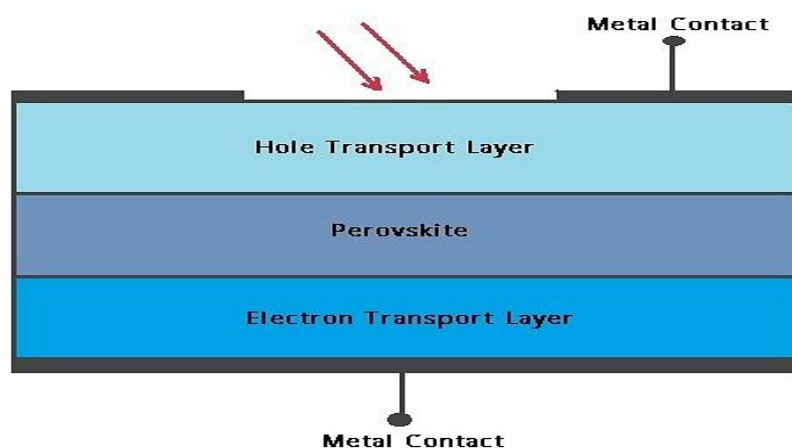


Fig 3.1: - Simulated Structure of Perovskite Solar Cell.

We have worked with planner inverted structure for all simulations. In the mid layer there exists Perovskite material. We have used CH₃NH₃PbI₃ (MAPbI₃) as absorber layer for all

structures for HTM we have considered two popular oxides which are recently being studied in various research work [15] for ETM, along the most popular materials TiO₂ we have explored the effect of other oxide based materials like ZnO and SnO₂ which are recently attracting attention of the PrSC researchers as effective contender of ETM.

3.2 SCAPS Input

3.2.1 Parameter Selection of Various Layers:

In SCAPS different properties of each layer need to be given as input shown in fig 3.2.

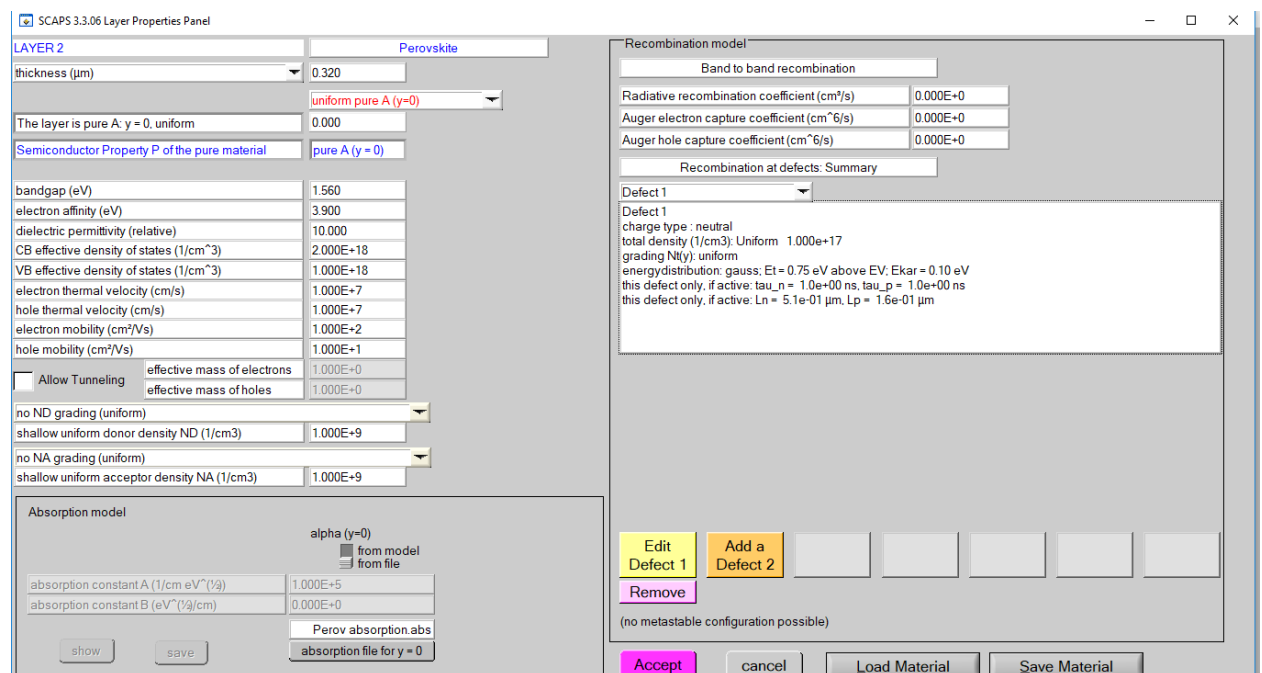


Fig 3.2: - SCAPS different properties of each layer.

The selection of each property plays the most significant role for a successful simulation result in this software. That's why we have given the most effort to select these properties. We have selected all properties/parameters from references journals considering proper conditions. Table-3.2 shown all parameters (with their references) for different layers used in our simulation.

Table 3.1: Properties of different layer used in SCAPS simulation.

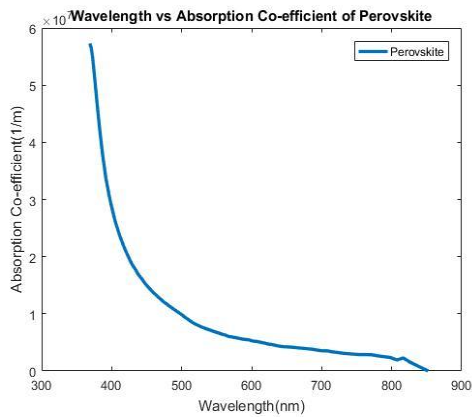
Properties	Cu ₂ O	NiOx	Perovskite	ZnO	SnO ₂	TiO ₂
Thickness(nm)	80	80	320	70	60	60
Bandgap(eV)	2.2	3.7	1.56	3.2	3.6	3.2
Affinity (eV)	3.3	2.1	3.9	4.1	4.07	4.2
Dielectric Permittivity	9.4	10.7	10	10	8	10
DOS of CB (1/cm ³)	8× 10 ¹⁷	2.8× 10 ¹⁹ [2× 10 ¹⁸	4.5× 10 ¹⁸	3.16× 10 ¹⁸ [16]	2.5× 10 ¹⁸
DOS of VB(1/cm ³)	1.8× 10 ¹⁹ [1.8× 10 ¹⁹	1× 10 ¹⁸ [51]	1× 10 ¹⁸	2.5× 10 ¹⁹	1× 10 ¹⁸
Electron mobility(cm ² /vs)	200	12	100	150	75[16]	0.7
Hole mobility (cm ² /vs)	90	25	10	1	0.1	0.1
Acceptor Concentration (1/cm ³)	1× 10 ¹⁶	2× 10 ¹⁴	1× 10 ⁰⁹	0	0	0
Donor Concentration	0	0	1× 10 ⁰⁹	1× 10 ¹⁶	1× 10 ¹⁸ [16]	9× 10 ¹⁷

3.2.2 Absorption Model:

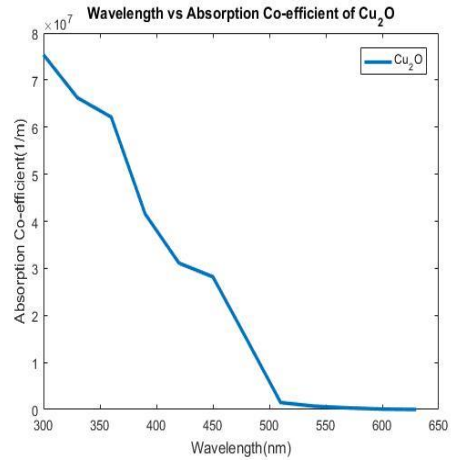
Absorption curve shows how light can get absorbed in a material. In SCAPS 3.3.06 there are two ways to give absorption information for a layer.

- Square Model → which uses $\alpha(\lambda) = (A + \frac{B}{h\nu})\sqrt{h\nu - E_g}$ formula to evaluate absorption coefficient .
- From input file → which takes a input file (.abs file to calculate absorption coefficient .

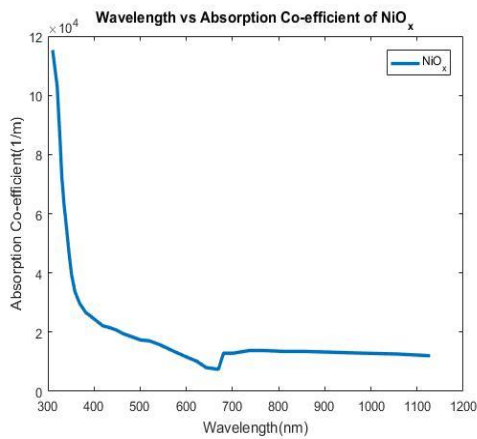
In this work we have chosen the second option because it gives more realistic view of absorption of a layer. For each layer the .abs file was prepared with data taken referred journal works. All absorption curves used for simulation are shown in fig 3.3



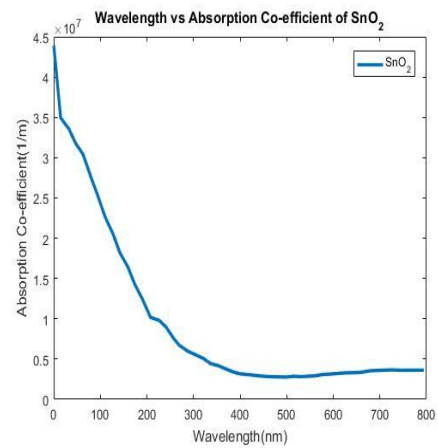
(a)



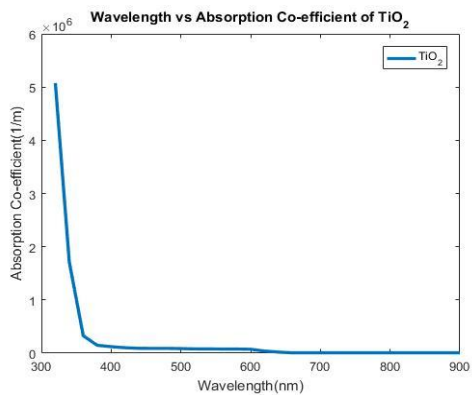
(b)



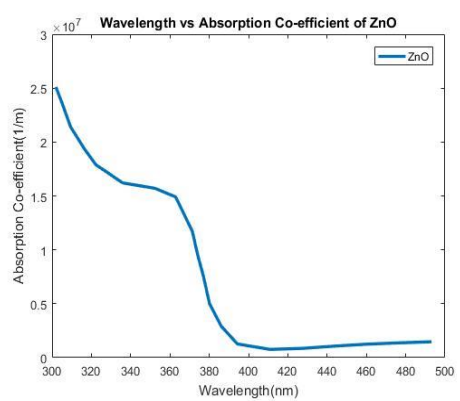
(c)



(d)



(e)



(f)

Fig: 3.3 Absorption Curve used in simulation for different layer: (a) MAPbI₃ Perovskite Layer (b) Cu₂O HTM Layer (c) NiO_x HTM Layer (d) SnO₂ ETL Layer (e)TiO₂ ETL Layer (f) ZnO ETL Layer

3.2.3 Contact:

For contact layer flat band has been used for both contact for all simulations.

3.2.4 Illumination:

For illumination solar spectrum of AM1.5G is used. Data is read through a file prepared from AM1.5G spectrum as shown as fig 3.4

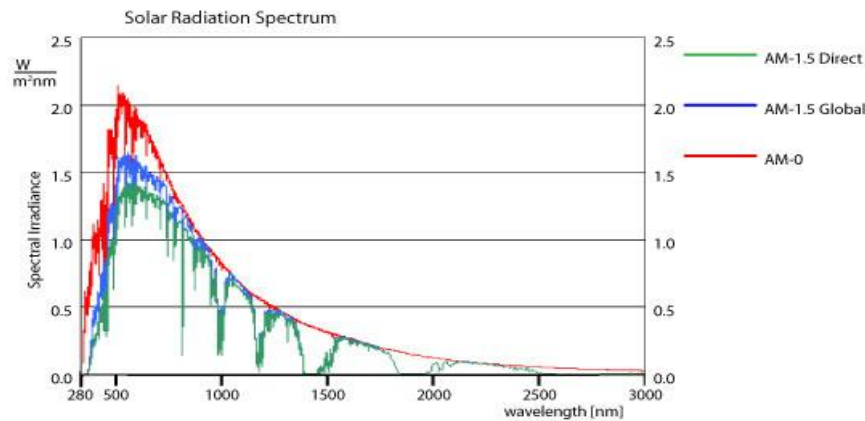


Fig 3.4 Solar-spectrum-of-AM 1.5 G [66]

As we have worked with inverted (p-i-n) structure. Light is given input from HTM side as shown in figure 3.1.

3.2.5 Bulk Defect and Interface State:

Defect plays one of the most important roles to limit the performance of a solar cell in real fabrication environment. Different fabrication limitations impose defects in the layers. To a reliable simulation result, these defects need to be considered accordingly. SCAPS 3306 gives us the option to incorporate these defects in two ways

- a. Bulk defects → represents materials defects due to fabrication limitations/inaccuracy.
- b. Interface defects → due to discontinuity of the structure at the conjunction of two layers.

Fig 3.5 shows the sample windows to give bulk and interface defects in SCAPS.

SCAPS 3.3.06 Defect Properties Panel

Defect 1 of Perovskite

defect type	Neutral	
capture cross section electrons (cm ²)	1.000E-15	
capture cross section holes (cm ²)	1.000E-15	
energetic distribution	Gauß	
reference for defect energy level Et	Above EV (SCAPS < 2.7)	
energy level with respect to Reference (eV)	0.750	
characteristic energy (eV)	0.100	

no Nt grading (uniform)

Nt total (1/cm ³)	uniform Nt	1.000E+17
Nt peak (1/eV/cm ³)	uniform Nt	5.642E+17

Optical capture of electrons From model From file

refractive index (n)	3.000
effective mass of electrons (rel.)	1.000E+0
effective field ratio	1.00E+0
cut off energy (eV)	10.00
optical electron capture cross sections file:	

Optical capture of holes From model From file

refractive index (n)	3.000
effective mass of holes (rel.)	1.000E+0
effective field ratio	1.00E+0
cut off energy (eV)	10.00
optical hole capture cross sections file:	

accept cancel

(a)

SCAPS 3.3.06 Interface Defect Properties Panel

Defect 1 of Perovskites / SnO2 interface

defect type	donor
capture cross section electrons (cm ²)	1.00E-17
capture cross section holes (cm ²)	1.00E-19
energetic distribution	single
reference for defect energy level Et	above the highest EV
energy with respect to Reference (eV)	0.600
characteristic energy (eV)	0.100
total density (integrated over all energies) (1/cm ²)	1.00E+14

Allow tunneling to interface traps

Relative mass of electrons	1.000E+0
Relative mass of holes	1.000E+0

accept cancel

(b)

Fig: 3.5 Sample window of SCAPS for defect input (a) Bulk defect (b) Interface defect.

In our simulation we have used defects in --

- a) MAPbI₃ (Perovskite) layer
- b) ETM layer
- c) Perovskite – ETM interface
- d) Perovskite – HTM interface

Table 3.2 shows the defect levels used in our simulation

Defect type	MAPbI ₃ layer bulk defect	ETM Layer bulk defect	ETM MAPbI ₃ interface	HTM MAPbI ₃ interface
Electron capture cross section (cm ²)	1×10^{-15}	1×10^{-15}	1×10^{-17}	1×10^{-19}
Hole capture cross section (cm ²)	1×10^{-15}	1×10^{-15}	1×10^{-19}	1×10^{-17}
Energetic distribution	Gauß	Gauß	Single	Single
Energy level with respect to Ref (eV)	0.75	0.5	0.6	0.6
Total defect density (cm ⁻³)	1×10^{17}	1×10^{15}	1×10^{14}	1×10^{14}

3.2.6 Selection of defect and interface Parameters.

Defect density of bulk or interface states are very carefully selected in our work to simulate the effect of fabrication environment so that our work represent authentication up to certain level.

For that we have considered a practical work [Tze-Bin Song et. al as the base of our work and tried to reproduce that result. The dimensional properties are set according to that work. Then bulk and interface defect levels are continuously changed on trial and error basis to

have a result closer to that work as well as the defect levels are kept at a reasonable range. The values used in Table 3.2 are thus chose finally.

Fig 3.6 shows the comparative result between our simulated work and the work of Tze-Bin Song et. Al.

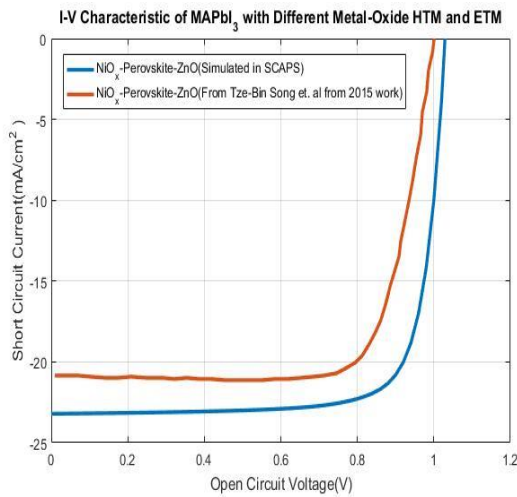


Fig 3.6: - Comparison between Experimental (fabrication) result from

Tze-Bin song et. al (2015) and our simulated work using SCAPS. The table shows the numerical values.

Parameters	NiO _x – Perovskite – ZnO(Simulation in SCAPS)	NiO _x – Perovskite – ZnO (from Tze-Bin song et. al (2015) work)
V _{oc} (v)	1.03	1.01[67]
J _{sc} (mA/cm ²)	23.206	21.00[67]
FF(%)	78.56	76.00[67]
η(%)	18.77	16.01[67]

From figure it is clearly evident how close our simulation result is with respect to experimental ones. We have got more J_{sc} than experimental value. this is due to the fact that the absorption data. We used may have not matched properly plus the extrapolation technique of SCAPS may have overstated the absorption than practical result. This have led to exaggerate result in efficiency as well. Nevertheless, the closeness of our result proves the satisfactory degree of validation of our work.

3.3 Simulation for Different Structure containing All-Metal-Oxide Transport Layers:

Once the validation of the simulation is achieved up to certain level, we simulated structure Fig: 3.1 for different metal oxide ETMs and HTMs. The choice of ETM & HTM was done by observing recent research interest. For ETM we have selected ZnO & SnO₂ besides mostly used ETM TiO₂ due to their fabrication feasibility and better electrical and

optical property. As HTM Cu_2O & NiO_x are chosen on the same sort of criteria. The whole methodology is summarized in the following figure, Fig 3.7

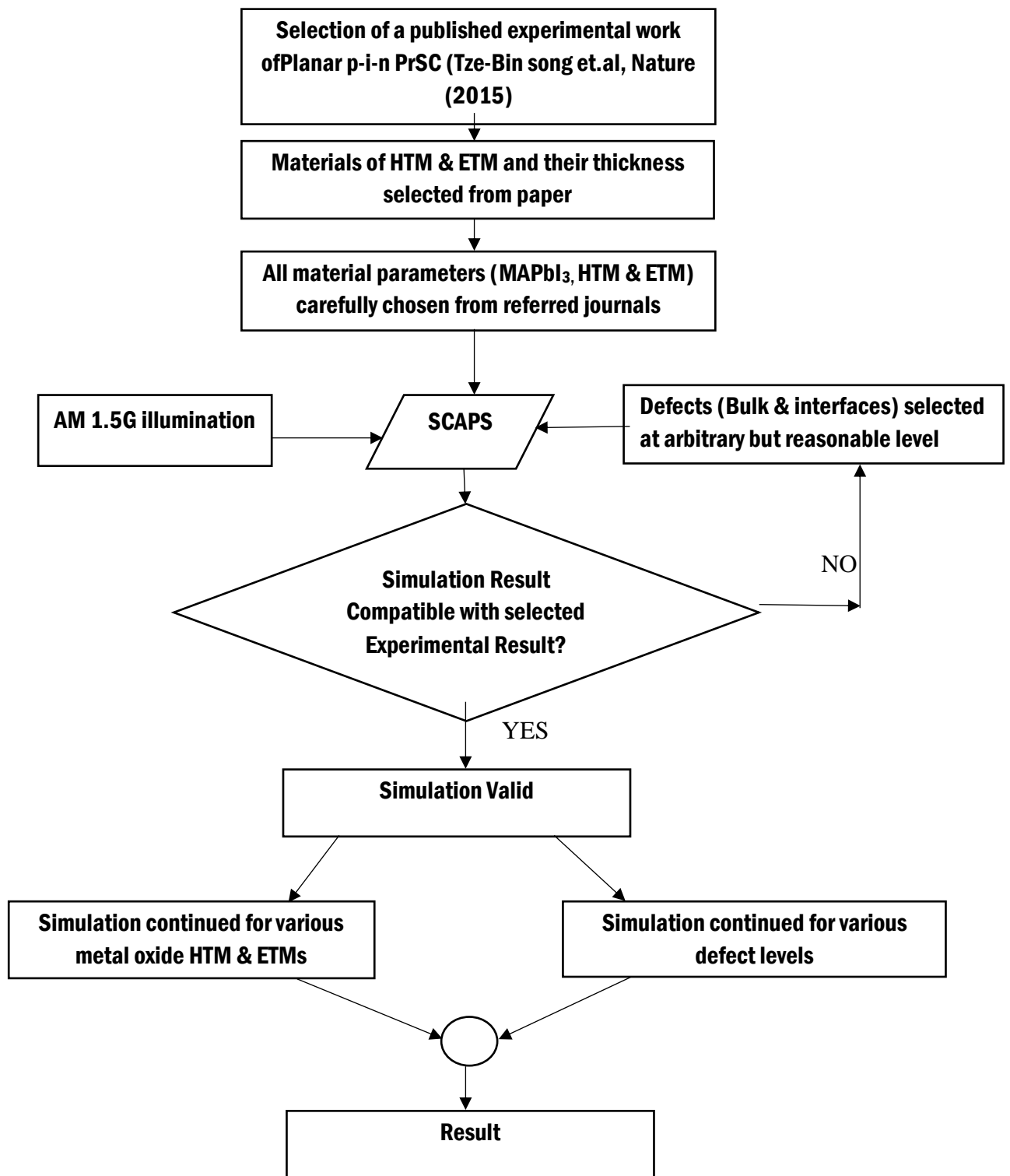


Fig 3.7: - flowchart of complete method of our work.

Chapter 4

Result and Discussion

Based on the methodology described in chapter 3 simulations are performed for six inverted planar perovskite structures. These structures are:

- i. NiO_x – MAPbI₃ – ZnO solar cell.
- ii. NiO_x – MAPbI₃ – TiO₂solar cell.
- iii. NiO_x – MAPbI₃ – SnO₂solar cell.
- iv. Cu₂O – MAPbI₃ – ZnO solar cell.
- v. Cu₂O – MAPbI₃ – TiO₂solar cell.
- vi. Cu₂O – MAPbI₃ – SnO₂solar cell.

The key properties of solar cell analyzed in this work for all variations are-

- Open circuit voltage, V_{oc} : maximum voltage which can appear across the solar cell without load
- Short Circuit Current, J_{sc} : maximum amount of current which can be draw from solar cell when the terminals are shorted
- Fill Factor: $FF = \frac{V_{max}J_{max}}{V_{oc}J_{sc}}$

Here, V_{max} = voltage of a cell at maximum power point.

J_{max} = Current density of the cell at that maximum power point.

This shows how non ideal a cell is.

- Efficiency: $Efficiency = \frac{P_{out}(electrical)}{P_{in}(solar)} \times 100\%$

This shows how much light energy is converted to electrical energy. All efficiency referred in this thesis work is power conversion efficiency (PCE)

The simulations were performed on all structures for four different situations.

- i. Analysis with Fixed Properties.
- ii. Analysis Varying Perovskite Thickness.
- iii. Analysis Varying Perovskite Bulk Defect Density.
- iv. Analysis Varying Perovskite-ETM Interface Defect Density.

4.1 Analysis with Fixed Properties:

Fig 4.1 and Fig 4.2 shows the I-V characteristic of solar cell structure as shown in Fig 3.1 for six structure containing different all oxide transport layer.

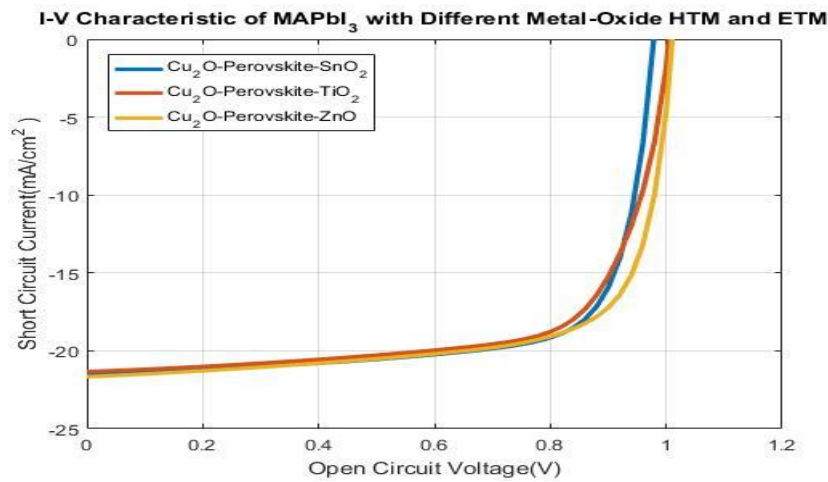


Fig 4.1: I-V characteristics of Cu₂O-MAPbI₃ structure for different ETMs.

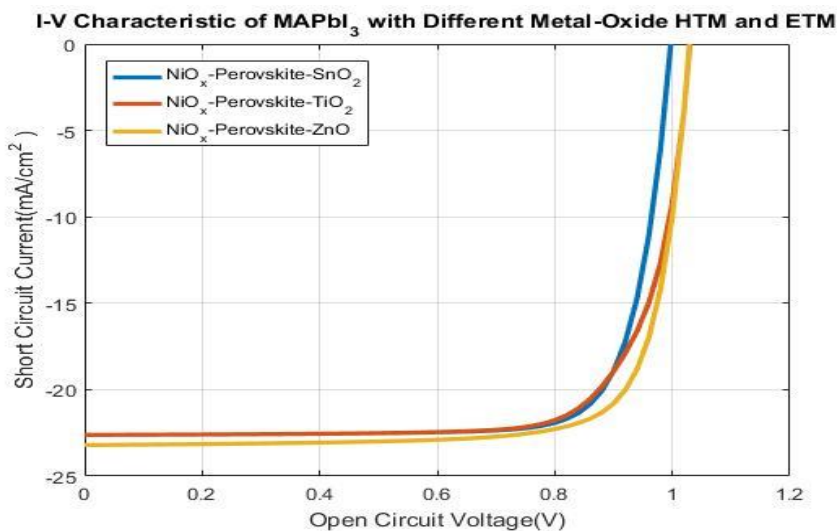


Fig 4.2: I-V characteristics of NiO_x-MAPbI₃ structure for different ETMs.

All simulations here are performed with high defect density (10^{17} cm^{-3}) of absorber layer and moderate interface defects (10^{14} cm^{-3}).

The key features of the cells are summarized in table 4.1

Table 4.1: Performance parameters of different perovskite solar cell structures.

Structure name	Open circuit voltage, V_{oc} (V)	Short circuit current, J_{sc} ($mA.cm^{-2}$)	Fill Factor, FF (%)	Efficiency, η (%)
Cu ₂ O-Perovskite- SnO ₂	0.9787	21.464758	74.01	15.55
Cu ₂ O-Perovskite- TiO ₂	1.0053	21.336338	70.53	15.13
Cu ₂ O-Perovskite- ZnO	1.0115	21.664595	71.60	15.69
NiO _x -Perovskite- SnO ₂	0.9976	22.619342	79.56	17.95
NiO _x -Perovskite- TiO ₂	1.0306	22.619436	75.99	17.71
NiO _x -Perovskite- ZnO	1.0298	23.205947	78.56	18.77

It is clearly evident from Fig. 4.1 and Fig. 4.2 that NiO_x based HTM are providing larger J_{sc} , FF and Efficiency than Cu₂O based HTM. Because Cu₂O(2.2eV) has smaller E_g than NiO_x(3.7eV) which makes Cu₂O to absorb more light resulting less light to pass towards perovskite layer.

For Cu₂O and NiO_x based structures SnO₂ is showing best performance in terms of FF but has poor performance in terms of V_{oc} at this defect and interface level. For the case of efficiency and short circuit current, all three structures of Cu₂O similar performance where as for NiO_x based structure, ZnO ETM is showing best performance. Cells containing TiO₂ ETM are having less efficiency than other three. From all these we can conclude that ZnO and SnO₂ are better contender for ETM than TiO₂ which is the widely used ETM for PrSC. But it should be mentioned that, this analysis is based on high defect bulk defect levels of absorber layer. The contrasting performances of these structures for a variety of defects and interface states are discussed Section 4.3 and 4.4 from which a concrete comparative conclusion can be drawn.

4.2 Analysis Varying Perovskite Thickness:

In this part we are intended to observe how the cell performances are influenced by thickness of absorber layer. For this purpose, the thickness of perovskite layer is varied from 200nm to 1500nm for all structures. The results are shown in Fig 4.3

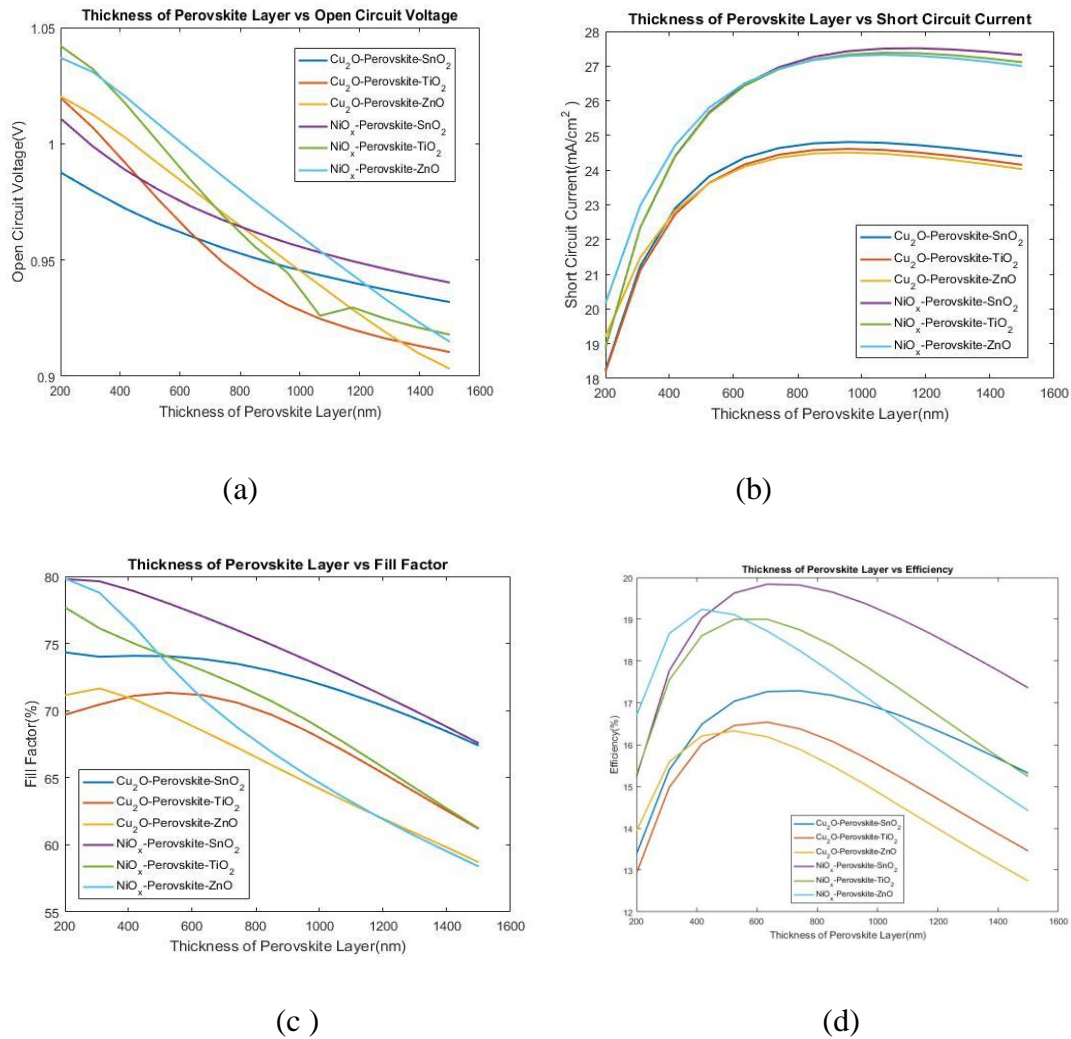


Fig: 4.3 Performance of perovskite solar cell for different perovskite thickness. (a) Thickness vs Open Circuit Voltage (b) Thickness vs Short Circuit voltage. (c) Thickness vs Fill Factor (d) Thickness vs Efficiency. [The bulk defect density is 10^{17} cm^{-3} , whereas the interface states are kept at 10^{14} cm^{-3} levels]

Fig 4.3(a) shows the variation of open circuit voltage as thickness increases. V_{oc} decreases for all structures. This is due to the carrier trapping effect of the defects. For SnO_2 based structure this effect is less prominent than others. On the other hand, there is a linear decay

of V_{ov} for ZnO based cells which signifies more sensitivity on thickness than other two ETM based cells.

Fig 4.3(b) shows that, short circuit current, J_{sc} increases as thickness increases and reaches saturation. So up-to certain thickness there will be more photo current above which not much improvement observed. As described earlier in Section 4.1, NiO_x base devices are showing better J_{sc} in which SnO_2 has better performance for layer thickness.

Fig 4.3(c) shows that, for the case of Fill Factor, FF decreases with increase of perovskite thickness of all structure NiO_x -Perovskite- SnO_2 showing less variations, whereas NiO_x -Perovskite-ZnO the FF decreases very rapidly with the thickness increase.

For the case of efficiency we can clearly see from Fig 4.3(d) that, for all structure efficiency increase up to a certain thickness and then decreases as thickness increases further. This is because with the increases of thickness absorption of light increases but at the same time layer resistance increases. That's why this we get an optimum thickness for the best performance for efficiency. Table 4.2 shows this optimum thickness all six structure.

Table 4.2: - Thickness for maximum efficiency

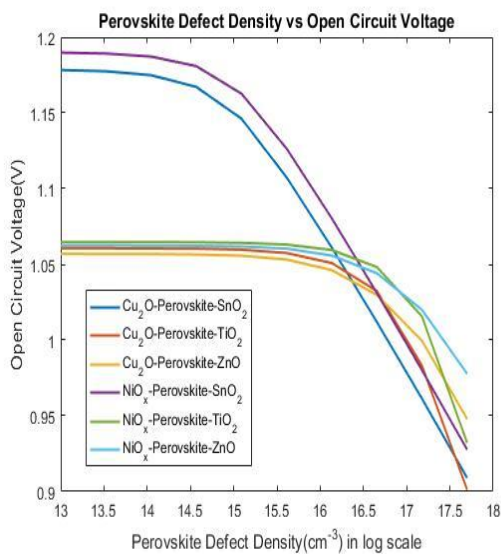
Structure name	Perovskite thickness for maximum efficiency, (nm)	Maximum efficiency, η (%)
Cu_2O -Perovskite- SnO_2	741.6	17.29
Cu_2O -Perovskite- TiO_2	633.2	16.54
Cu_2O -Perovskite- ZnO	524.4	16.33
NiO_x -Perovskite- SnO_2	633.2	19.84
NiO_x -Perovskite- TiO_2	633.2	19
NiO_x -Perovskite- ZnO	416.6	19.24

For the table it is clearly evident that NiO_x based devices are having better efficiency out of which cell with SnO_2 ETM is showing the best performance. For ZnO ETM, efficiency reduces more rapidly than others for both HTMs. Another observation is also evident that, ZnO based cells are having less optimum thickness than other two ETM based cells (around

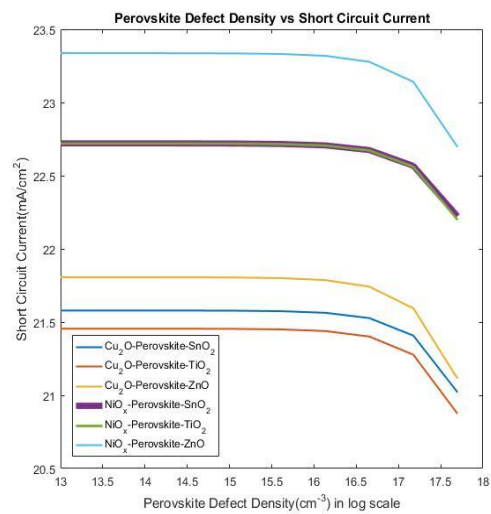
150-200nm less thickness). This is a significant finding because it shows cells containing ZnO as ETM can be made thinner than others with comparable performance.

4.3 Analysis Varying Perovskite Bulk Defect Density:

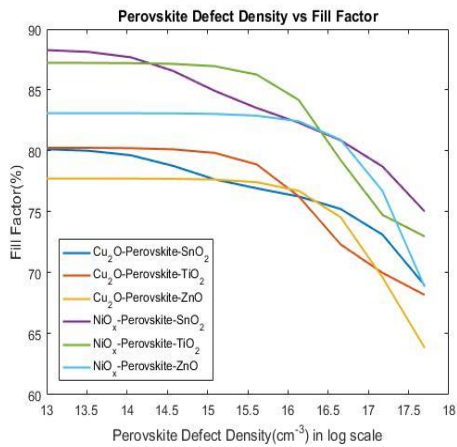
In this section, we are putting our focus on one of the most performance limiting factors for a solar cell – defects in absorber layer. Defects are the result of fabrication imperfections and limitations. These levels acts as ‘trap centers’ which causes carriers to recombine commonly known as Shockley-Read-Hall (SRH) recombination. This decreases carrier lifetime resulting less photocurrent and less efficient cells. To observe this effect, The defect density of perovskite layer(bulk defect) is varied from $1 \times 10^{13} \text{ cm}^{-3}$ to $5 \times 10^{17} \text{ cm}^{-3}$ and the performance are evaluated as shown in Fig 4.4



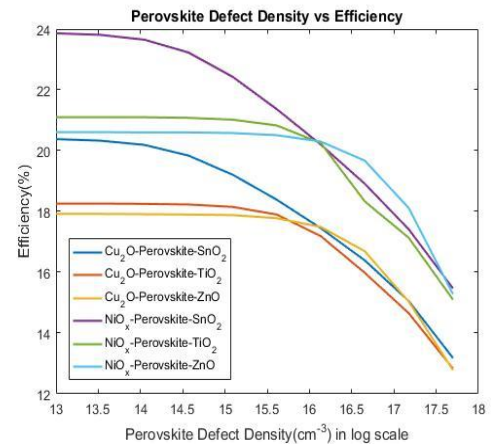
(a)



(b)



(c)



(d)

Fig 4.4: - Performance of perovskite solar cell for different perovskite defect density (a) defect density vs Open Circuit Voltage (b) defect density vs Short Circuit voltage. (c) defect density vs Fill Factor (d) defect density vs Efficiency [thickness of absorber layer was kept at 320nm]

As expected all properties shown degraded performance as defect increases. With the increase of defect, more photo generated carriers get trapped. Resulting less carrier density for photocurrent.

From figure 4.4(a) we can see for all structure other than SnO₂ based cells showing similar effect on V_{oc} for the variation for defects. Up to certain level (around $5 \times 10^{16} \text{ cm}^{-3}$ defect density) there is almost no change in V_{oc} after that V_{oc} decreases. This signifies that, cells with ZnO and TiO₂ ETMs are showing better stability for open circuit voltage from low to moderate defect levels. Thus it can be concluded that, bulk defects has lesser effect on open circuit voltage of PrSCs.

But for SnO₂, the situation is very different. For low level defect SnO₂ cells are showing highest V_{oc} for both Cu₂O and NiO_x HTMs. It is expected due to better conduction band maximum (CBM) band alignment as shown in Fig 4.5. CB offset for SnO₂ is 0.17eV where as that for ZnO and TiO₂ are 0.2eV and 0.3eV respectively.

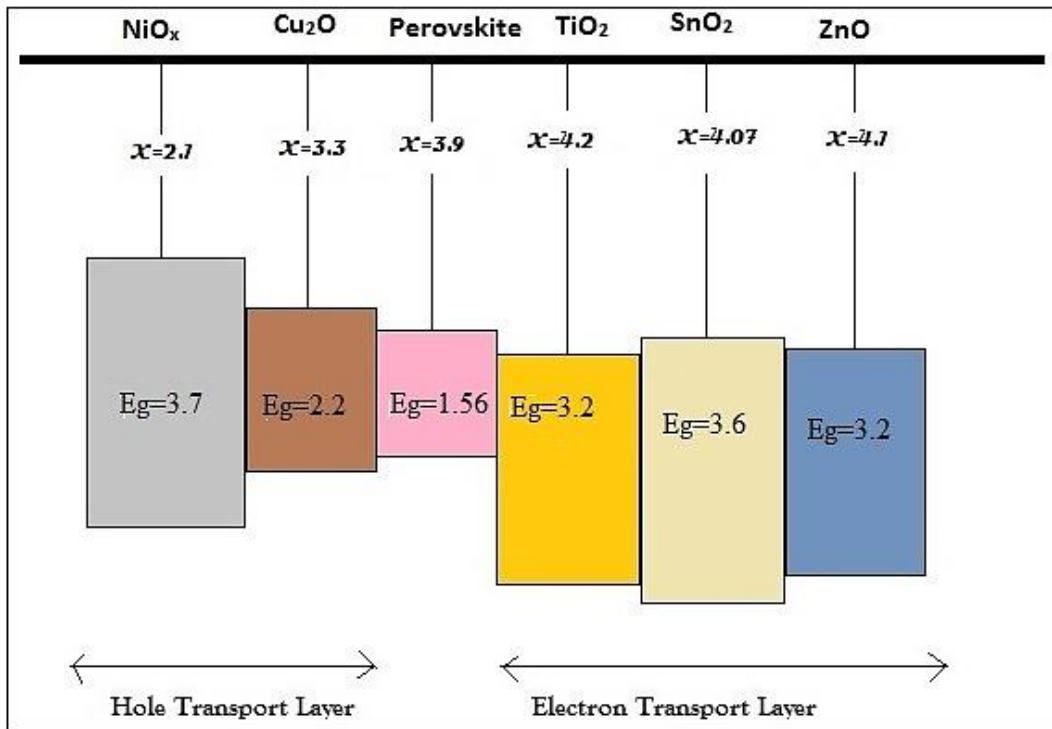


Fig 4.5: - Band alignment of different materials used in simulation.

But as defect increases, those cells becomes more sensitive than other and V_{oc} decreases rapidly and becomes even lower than others. So, SnO₂ devices are showing less susceptible on defects than others in terms of V_{oc} .

Fig 4.3(b) shows that for J_{sc} all devices are showing similar performance that up to certain defect levels there is no change in J_{sc} but above that J_{sc} decreases rapidly.

Fig 4.3(c) shows the variation of FF with defect density of perovskite. FF is significantly affected for moderate to high defect densities for all devices. ZnO based cells are showing more robust FF than others. On the other hand, SnO₂ based devices gives more instability with defect changes than others. All though TiO₂ based devices are having more stable FF than SnO₂ based device, these show more rapidly decrease than SnO₂.

From efficiency vs defect density graph from Fig 4.4 (d) there are some interesting observations obtained. For SnO₂ based devices efficiency has more effect on defect levels than others. All though ZnO based devices have lower efficiency in low defect levels at high defect density ZnO cells are showing best performance than SnO₂& TiO₂ based

devices specially with NiO_x HTM. So, ZnO based cells are better in terms of stability and high defect level operations. This is indeed a very important finding of this work.

4.4 Analysis Varying Perovskite-ETM Interface Defect Density:

Interface defects are the result of discontinuity in structure at the conjunction of two layers. As carrier passes from one layer to another these defects recombine carriers resulting reduced carrier density. Thus interface states reduce performance. In this part, we are showing the effect of efficiency of PSC on perovskite-ETM interface defects.

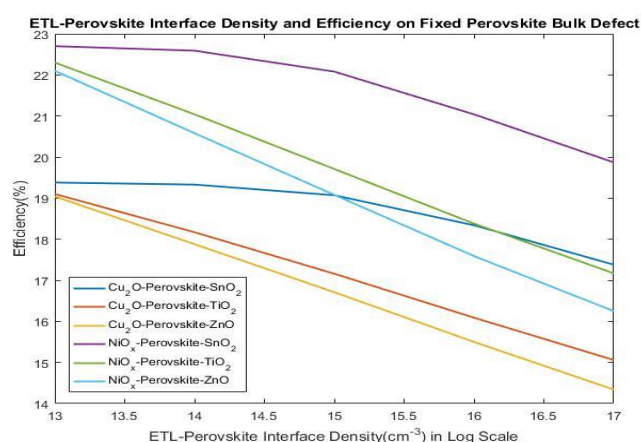
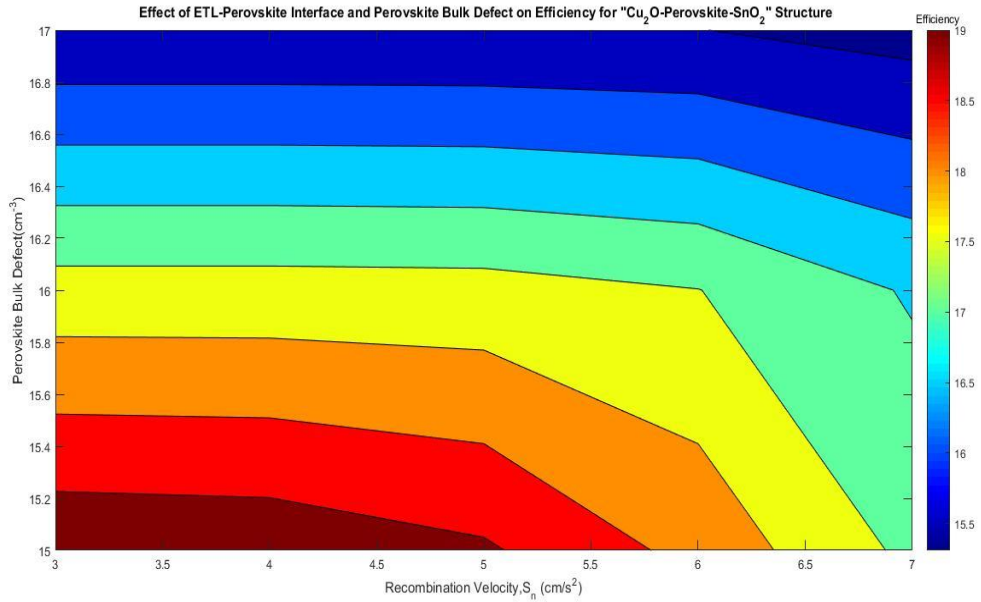


Fig 4.6: Analysis of Perovskite Solar Cell for Different Perovskite ETL interface State at Bulk Defect 10^{15} cm^{-3}

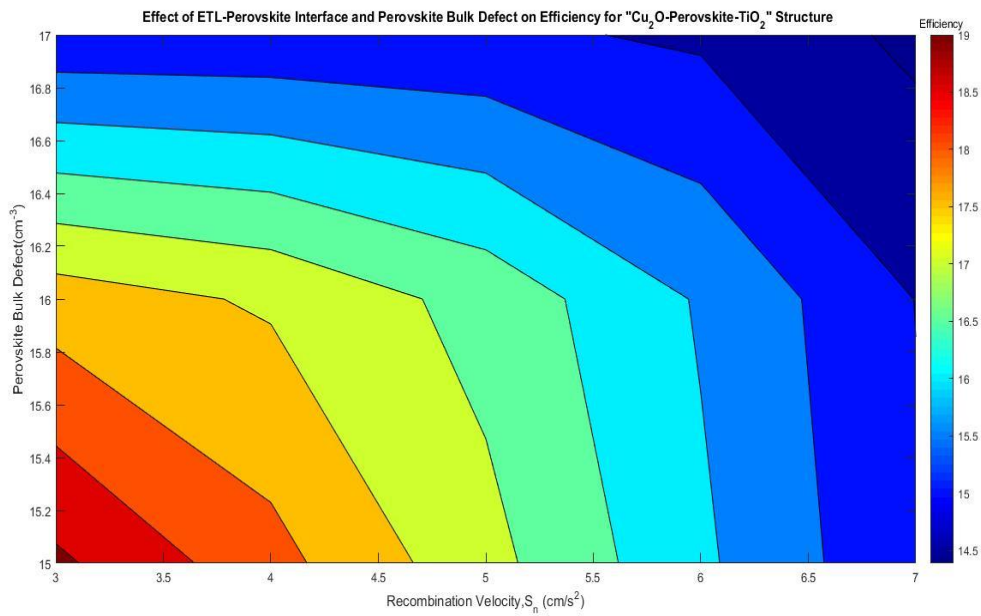
Fig 4.6 shows the variation of efficiency of all six solar cell we studied with the increase of interface state densities at perovskite bulk defect at 10^{15} cm^{-3} level and as expected efficiency decreases with the increase of interface states. For ZnO and TiO₂ based devices there occurs linear decrease all though the decrement rate is higher for ZnO devices. On the other hand, SnO₂ based devices shows more tolerance than others. For these cells the decrease of efficiency is at slower rate than others. So, at bulk defect at 10^{15} cm^{-3} ; SnO₂ based cells are showing more stable performance where as ZnO based cells are more prone to such interface states.

Next, we analyzed the SC structure for the cumulative effect of bulk defect and interface states. We have varied bulk defects from 10^{15} to 10^{17} cm^{-3} and interface states from 10^{13} to 10^{17} cm^{-3} and observed the effect of these on the cell efficiencies. Fig 4.7 shows

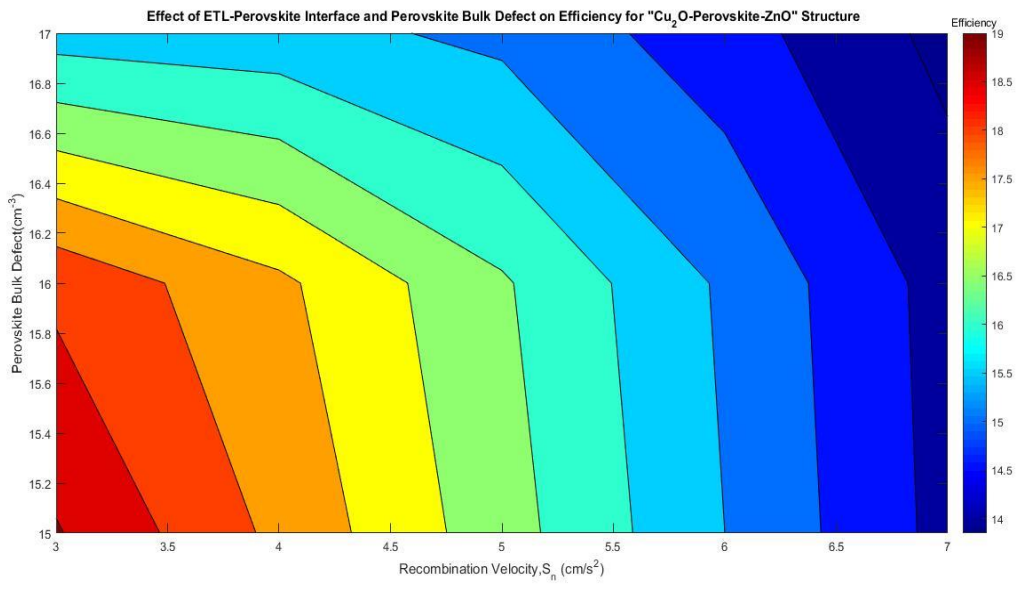
the contour plots for the six cell structures for the combined variation of bulk defects and interface states.



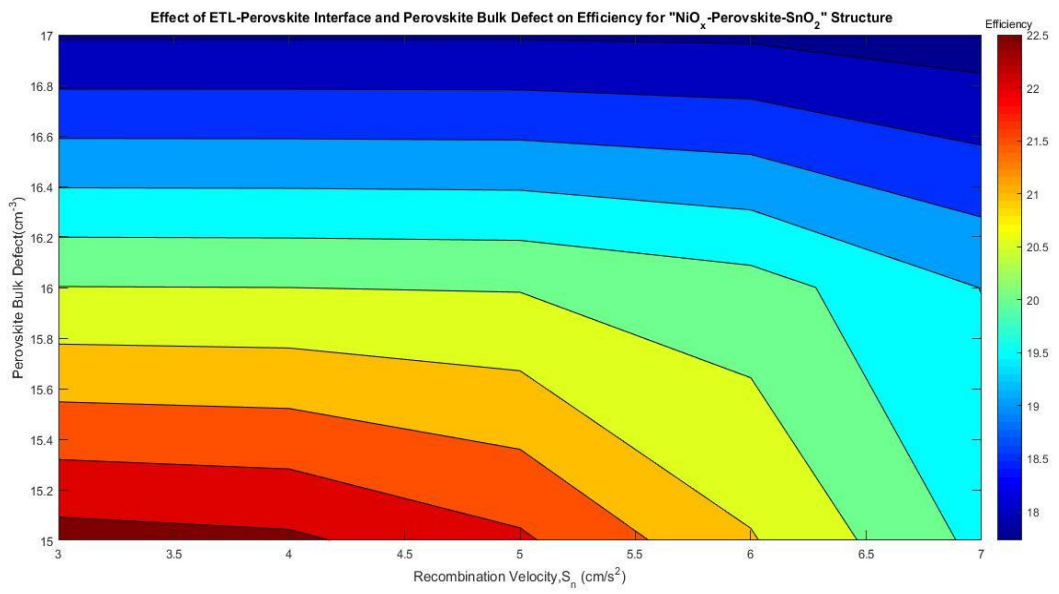
(a)



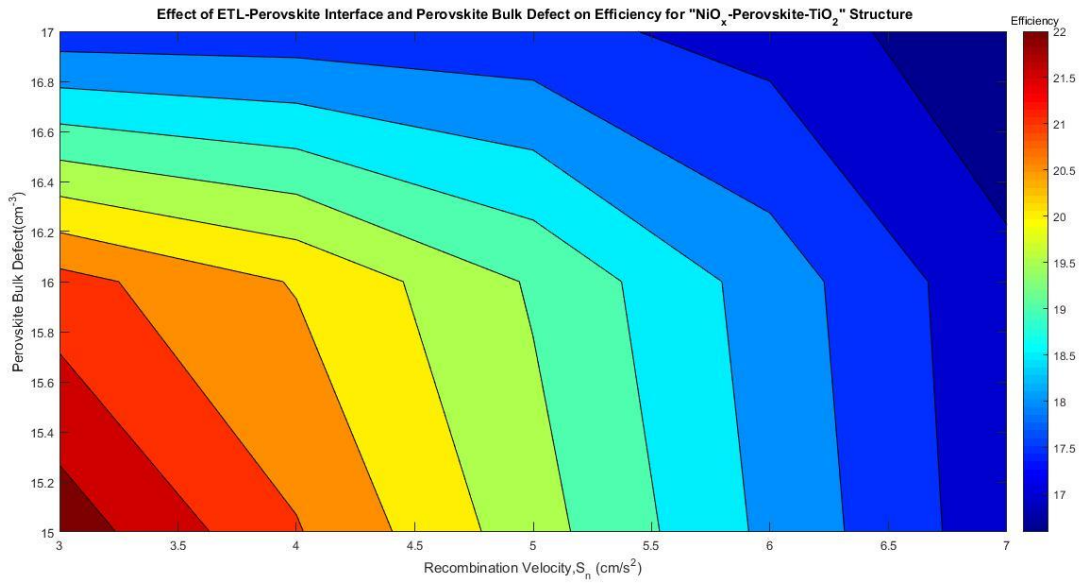
(b)



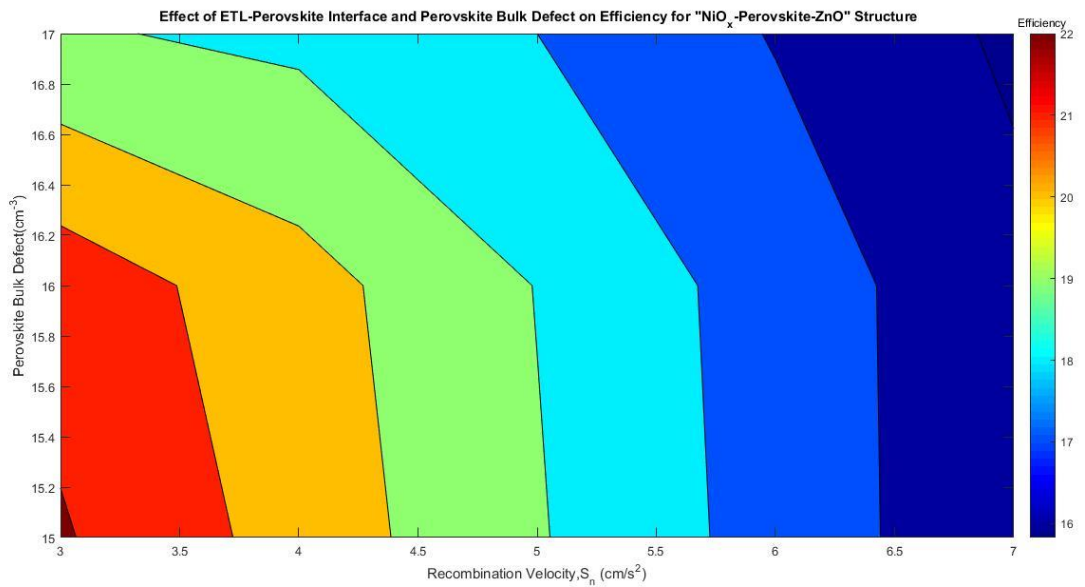
(c)



(d)



(e)



(f)

Fig 4.7: Effect of ETL-Perovskite Interface and Perovskite bulk defect on Efficiency for different Structure. (a) Cu₂O- Perovskite- ZnO Structure. (b) Cu₂O- Perovskite- TiO₂ Structure (c) Cu₂O - Perovskite- SnO₂ Structure. (d) NiO_x - Perovskite- ZnO Structure. (e) NiO_x - Perovskite- TiO₂ Structure (f) NiO_x - Perovskite- SnO₂ Structure.

The interface states are represented here in terms of interface recombination rates/velocity, $S_n(\text{cm/s})$;

$$S_n = \delta_n N_{in} V_{th}$$

Where,

δ_n = electron captures cross section

N_{in} = interface defect density

V_{th} = thermal velocity of electrons

For the analysis we have considered the effect on holes to be very negligible as in perovskite-ETM interface the main current component is due to electron flow.

For the SnO_2 -based devices as in Fig 4.7(a) and 4.7(d) it is clear that for higher defect levels there is a very few effect on interface states on cell efficiencies. Here cell performance is dominated by bulk defect. On the other hand, for low levels of bulk defect efficiency remains stable up to certain interface states above which there occurs decrease in efficiency.

TiO_2 based cells shows more sensitive on interface states than SnO_2 based devices. In such cells, as shown in Fig 4.7(b) and Fig 4.7(e) even in higher defect levels there occurs decrease in efficiency as interface recombination increases.

ZnO based cells shows the most sensitivity on interface states than all. For these cells interface states dominate the efficiency of solar cell as shown in Fig 4.7(c) and Fig 4.7(f).

Now, if we shift our focus on the variation of HTM (Cu_2O & NiO_x) it is very evident from the contour plots that, all though Cu_2O based devices are having less efficiency than NiO_x based cells, they are showing more tolerance to defect levels than NiO_x ones. For a constant interface states there occurs more variation in efficiency for NiO_x cells than Cu_2O ones. But there is an exception for ZnO-NiO_x cells. Here the cells are more tolerant on bulk defect level and interface states.

Chapter 5

Conclusion

In this work, we have presented a simulation based study of $\text{CH}_3\text{NH}_3\text{PbI}_3$ (MAPbI₃) perovskite solar cell (PrSC) with all-metal-oxide transport layers in inverted planar structure (p-i-n structure) using 1D simulation software SCAPS. For hole transport material (HTM) we have chosen Cu_2O and NiO_x . On the other hand, ZnO and SnO_2 are selected for electron transport material along with the mostly studied ETM TiO_2 . For all six structures several studies are performed for the variation of perovskite layer thickness and bulk defect as well as perovskite-ETM interface defect states to analyze their performances. The main findings of this work is summarized below.

- i. At higher defect levels (defect density 10^{17} cm^{-3}) the efficiency of the devices are found in the range of 15 – 19% which is not impractical to achieve for inverted planar PrSC. The open circuit voltages are found in the range of 0.9V to 1.05V with fill factor to be in 70 – 80%. All these results are in the feasible range which shows the validation of this simulation based work.
- ii. Although the main focus is given on the behavior of ETM variation in this thesis work (that's why no defect was put to HTM layer and moderate interface defect level was given to perovskite-HTM interface), the superiority of NiO_x as HTM is clearly visible over Cu_2O . For all ETMs, cells with NiO_x are showing better performance. This is due to less optical transparency of Cu_2O .
- iii. In spite of TiO_2 being the mostly studied ETM for PrSC, in our simulation SnO_2 based cells have showed the better efficiency, FF and short circuit current than others specially at the lower to mid defect levels. They have also shown more robustness on interface states variations as well. But for open circuit voltage the behavior with defects is not satisfactory at higher levels. For lower defect states V_{OC} is quite higher than others but it decreases very rapidly with the increase of defect levels and eventually go below others. Overall, SnO_2 is showing promising performance as ETM and can be thought of a better alternative than TiO_2 .
- iv. While cells with SnO_2 ETM are having poorer performance for higher defect levels, cells with ZnO ETM has defeated other twos in terms of tolerance to absorber bulk defects although their performance is quite similar if not worse

than TiO_2 . They have provided a stable efficiency than others in terms of defect variation. Even at higher levels efficiency of ZnO based cells are superior than other two. Moreover, the ZnO- NiO_x cell have shown the most steadiness for both interface states and bulk defects. Furthermore, ZnO cells have shown least optimum thickness of all and higher short circuit current for all defect levels. The underlying reason behind this should be the higher carrier concentration leading to higher conductivity. So it can be concluded that ZnO like SnO_2 can also be a better contender for TiO_2 , specially for higher current.

5.1 Limitation:

Limitation of the simulation process to work with SCAPS 1D program the results we obtained are constant to the following limitations.

- i. We worked with only the active layers of perovskite solar cell. We ignored the effect of substrate layer below ETM layer generally used indium doped Tin Oxide(ITO) or fluorine doped Tin Oxide(FTO). This ignores the resistive and optical absorption effect imposed by this layer.
- ii. Only one defect levels were used for each layer which deviates the result from practical situation up to certain extent.
- iii. All contacts are considered as flat-band. This is ignoring the effect of contact layer barrier which effects device performance.
- iv. No generation model was given as input default generation profile was used.
- v. For some few cases extrapolation scheme done to absorption file by SCPAS leads to some impractical situation.

5.2 Future work:

Multivalent defects, incorporation of FTO/ITO layers and various conduction levels of transport layers can be incorporated in simulation for more realistic results .Other unconventional transparent conducting oxides can be studied similarly as transport layers for PrSCs. Furthermore, perovskite layers other than MAPbI_3 can be studied.

Appendix-1

Data Table from Simulation:

Table 01 Comparison between Experimental (fabrication) result from Tze-Bin song et. al (2015) and our simulated work using SCAPS

Table: 01.a NiO_x–Perovskite – ZnO(Simulation in SCAPS)

Open Circiut Voltage, V _{oc} (V)	Short Circuit Current(mA/cm ²)
0.00E+00	-2.32E+01
2.00E-02	-2.32E+01
4.00E-02	-2.32E+01
6.00E-02	-2.32E+01
8.00E-02	-2.32E+01
1.00E-01	-2.32E+01
1.20E-01	-2.32E+01
1.40E-01	-2.32E+01
1.60E-01	-2.32E+01
1.80E-01	-2.32E+01
2.00E-01	-2.32E+01
2.20E-01	-2.31E+01
2.40E-01	-2.31E+01
2.60E-01	-2.31E+01
2.80E-01	-2.31E+01
3.00E-01	-2.31E+01
3.20E-01	-2.31E+01
3.40E-01	-2.31E+01
3.60E-01	-2.31E+01
3.80E-01	-2.31E+01
4.00E-01	-2.31E+01
4.20E-01	-2.31E+01
4.40E-01	-2.30E+01
4.60E-01	-2.30E+01
4.80E-01	-2.30E+01
5.00E-01	-2.30E+01

5.20E-01	-2.30E+01
5.40E-01	-2.30E+01
5.60E-01	-2.29E+01
5.80E-01	-2.29E+01
6.00E-01	-2.29E+01
6.20E-01	-2.29E+01
6.40E-01	-2.28E+01
6.60E-01	-2.28E+01
6.80E-01	-2.28E+01
7.00E-01	-2.27E+01
7.20E-01	-2.27E+01
7.40E-01	-2.26E+01
7.60E-01	-2.25E+01
7.80E-01	-2.24E+01
8.00E-01	-2.23E+01
8.20E-01	-2.21E+01
8.40E-01	-2.19E+01
8.60E-01	-2.17E+01
8.80E-01	-2.13E+01
9.00E-01	-2.08E+01
9.20E-01	-2.00E+01
9.40E-01	-1.88E+01
9.60E-01	-1.70E+01
9.80E-01	-1.42E+01
1.00E+00	-9.98E+00
1.02E+00	-3.88E+00
1.04E+00	4.69E+00

Table 01.b NiO_x–Perovskite – ZnO (from Tze-Bin song et. Al, 2015 work)

Open Circiut Voltage, V _{oc} (V)	Short Circuit Current(mA/cmcm ²)
0.008999	-20.8399
0.039115	-20.8399
0.069231	-20.8399
0.101675	-20.9121
0.14107	-20.9843
0.175819	-20.9843
0.208239	-20.9121
0.247633	-20.9843
0.291649	-20.9843
0.321777	-21.0564
0.354197	-20.9843
0.386642	-21.0564
0.419074	-21.0564
0.453835	-21.1286
0.483951	-21.1286
0.514067	-21.1286
0.551132	-21.1286
0.583553	-21.0564
0.618302	-21.0564
0.653039	-20.9843
0.685459	-20.9121
0.713246	-20.8399
0.745654	-20.6955
0.768771	-20.4068
0.794193	-20.0459
0.812653	-19.6129
0.831064	-18.8911
0.847159	-18.1693
0.860937	-17.4475

0.874654	-16.3648
0.886055	-15.2822
0.8952	-14.5604
0.908917	-13.4777
0.913392	-12.5394
0.924756	-11.2402
0.93384	-10.1575
0.94518	-8.71391
0.954215	-7.34252
0.965567	-5.97113
0.969957	-4.52756
0.981333	-3.30052
0.985748	-2.00131
0.997124	-0.77428
1.003818	0.74147
1.010476	2.473753

Table 02 Analysis with Fixed Properties:

Table 2.a Cu₂O-Perovskite-SnO₂

Open Circiut Voltage, V _{oc} (V)	Short Circuit Current(mA/cm ²)
0.62	-2.02E+01
0.64	-2.01E+01
0.66	-2.00E+01
0.68	-1.99E+01
0.7	-1.99E+01
0.72	-1.98E+01
0.74	-1.97E+01
0.76	-1.95E+01
0.78	-1.94E+01
0.8	-1.92E+01

0.82	-1.89E+01
0.84	-1.85E+01
0.86	-1.80E+01
0.88	-1.72E+01
0.9	-1.59E+01
0.92	-1.41E+01
0.94	-1.12E+01
0.96	-6.63E+00
0.98	5.25E-01
1	8.90E+00
0.62	-2.02E+01

Table 2.b Cu₂O -Perovskite-TiO₂

Open Circiut Voltage, V _{oc} (V)	Short Circuit Current(mA/cm ²)
0	-2.13E+01
0.02	-2.13E+01
0.04	-2.13E+01
0.06	-2.12E+01
0.08	-2.12E+01
0.1	-2.12E+01
0.12	-2.12E+01
0.14	-2.11E+01
0.16	-2.11E+01
0.18	-2.10E+01
0.2	-2.10E+01
0.22	-2.10E+01
0.24	-2.09E+01
0.26	-2.09E+01
0.28	-2.08E+01
0.3	-2.08E+01
0.32	-2.07E+01

0.34	-2.07E+01
0.36	-2.07E+01
0.38	-2.06E+01
0.4	-2.05E+01
0.42	-2.05E+01
0.44	-2.04E+01
0.46	-2.04E+01
0.48	-2.03E+01
0.5	-2.03E+01
0.52	-2.02E+01
0.54	-2.02E+01
0.56	-2.01E+01
0.58	-2.00E+01
0.6	-2.00E+01
0.62	-1.99E+01
0.64	-1.98E+01
0.66	-1.97E+01
0.68	-1.97E+01
0.7	-1.96E+01
0.72	-1.95E+01
0.74	-1.93E+01
0.76	-1.92E+01
0.78	-1.90E+01
0.8	-1.88E+01
0.82	-1.84E+01
0.84	-1.80E+01
0.86	-1.73E+01
0.88	-1.64E+01
0.9	-1.52E+01
0.92	-1.38E+01
0.94	-1.20E+01
0.96	-9.69E+00

0.98	-6.57E+00
1	-1.80E+00
1.02	6.08E+00

Table 2.c Cu₂O -Perovskite-ZnO

Open Circiut Voltage, V _{oc} (V)	Short Circuit Current(mA/cm ²)
0	-2.17E+01
0.02	-2.16E+01
0.04	-2.16E+01
0.06	-2.16E+01
0.08	-2.15E+01
0.1	-2.15E+01
0.12	-2.14E+01
0.14	-2.14E+01
0.16	-2.14E+01
0.18	-2.13E+01
0.2	-2.13E+01
0.22	-2.12E+01
0.24	-2.12E+01
0.26	-2.11E+01
0.28	-2.11E+01
0.3	-2.10E+01
0.32	-2.10E+01
0.34	-2.09E+01
0.36	-2.09E+01
0.38	-2.08E+01

0.4	-2.08E+01
0.42	-2.07E+01
0.44	-2.07E+01
0.46	-2.06E+01
0.48	-2.06E+01
0.5	-2.05E+01
0.52	-2.04E+01
0.54	-2.04E+01
0.56	-2.03E+01
0.58	-2.03E+01
0.6	-2.02E+01
0.62	-2.01E+01
0.64	-2.00E+01
0.66	-2.00E+01
0.68	-1.99E+01
0.7	-1.98E+01
0.72	-1.97E+01
0.74	-1.96E+01
0.76	-1.94E+01
0.78	-1.93E+01
0.8	-1.91E+01
0.82	-1.88E+01
0.84	-1.86E+01
0.86	-1.82E+01
0.88	-1.78E+01
0.9	-1.72E+01
0.92	-1.64E+01
0.94	-1.51E+01
0.96	-1.32E+01
0.98	-9.95E+00
1	-4.65E+00
1.02	4.21E+00

Table 2.d NiO_x-Perovskite-SnO₂

Open Circiut Voltage, V _{oc} (V)	Short Circuit Current(mA/cm ²)
0	-2.26E+01
0.02	-2.26E+01
0.04	-2.26E+01
0.06	-2.26E+01
0.08	-2.26E+01
0.1	-2.26E+01
0.12	-2.26E+01
0.14	-2.26E+01
0.16	-2.26E+01
0.18	-2.26E+01
0.2	-2.26E+01
0.22	-2.26E+01
0.24	-2.26E+01
0.26	-2.26E+01
0.28	-2.26E+01
0.3	-2.26E+01
0.32	-2.26E+01
0.34	-2.26E+01
0.36	-2.26E+01
0.38	-2.26E+01
0.4	-2.26E+01
0.42	-2.25E+01
0.44	-2.25E+01
0.46	-2.25E+01
0.48	-2.25E+01
0.5	-2.25E+01

0.52	-2.25E+01
0.54	-2.25E+01
0.56	-2.25E+01
0.58	-2.25E+01
0.6	-2.25E+01
0.62	-2.25E+01
0.64	-2.24E+01
0.66	-2.24E+01
0.68	-2.24E+01
0.7	-2.24E+01
0.72	-2.23E+01
0.74	-2.23E+01
0.76	-2.22E+01
0.78	-2.21E+01
0.8	-2.19E+01
0.82	-2.17E+01
0.84	-2.14E+01
0.86	-2.08E+01
0.88	-2.01E+01
0.9	-1.89E+01
0.92	-1.72E+01
0.94	-1.47E+01
0.96	-1.11E+01
0.98	-6.04E+00
1	9.28E-01

Table 2.e NiO_x-Perovskite-TnO₂

Open Circiut Voltage, V _{oc} (V)	Short Circuit Current(mA/cm ²)
0	-2.26E+01
0.02	-2.26E+01
0.04	-2.26E+01

0.06	-2.26E+01
0.08	-2.26E+01
0.1	-2.26E+01
0.12	-2.26E+01
0.14	-2.26E+01
0.16	-2.26E+01
0.18	-2.26E+01
0.2	-2.26E+01
0.22	-2.26E+01
0.24	-2.26E+01
0.26	-2.26E+01
0.28	-2.26E+01
0.3	-2.26E+01
0.32	-2.26E+01
0.34	-2.26E+01
0.36	-2.26E+01
0.38	-2.26E+01
0.4	-2.25E+01
0.42	-2.25E+01
0.44	-2.25E+01
0.46	-2.25E+01
0.48	-2.25E+01
0.5	-2.25E+01
0.52	-2.25E+01
0.54	-2.25E+01
0.56	-2.25E+01
0.58	-2.25E+01
0.6	-2.25E+01
0.62	-2.24E+01
0.64	-2.24E+01
0.66	-2.24E+01
0.68	-2.24E+01

0.7	-2.23E+01
0.72	-2.23E+01
0.74	-2.22E+01
0.76	-2.21E+01
0.78	-2.20E+01
0.8	-2.18E+01
0.82	-2.15E+01
0.84	-2.11E+01
0.86	-2.05E+01
0.88	-1.98E+01
0.9	-1.89E+01
0.92	-1.79E+01
0.94	-1.66E+01
0.96	-1.50E+01
0.98	-1.27E+01
1	-9.19E+00
1.02	-3.90E+00
1.04	4.05E+00

Table 2.f NiO_x-Perovskite-ZnO

Open Circiut Voltage, V _{oc} (V)	Short Circuit Current(mA/cm ²)
0	-2.32E+01
0.02	-2.32E+01
0.04	-2.32E+01
0.06	-2.32E+01
0.08	-2.32E+01
0.1	-2.32E+01
0.12	-2.32E+01
0.14	-2.32E+01
0.16	-2.32E+01
0.18	-2.32E+01

0.2	-2.32E+01
0.22	-2.31E+01
0.24	-2.31E+01
0.26	-2.31E+01
0.28	-2.31E+01
0.3	-2.31E+01
0.32	-2.31E+01
0.34	-2.31E+01
0.36	-2.31E+01
0.38	-2.31E+01
0.4	-2.31E+01
0.42	-2.31E+01
0.44	-2.30E+01
0.46	-2.30E+01
0.48	-2.30E+01
0.5	-2.30E+01
0.52	-2.30E+01
0.54	-2.30E+01
0.56	-2.29E+01
0.58	-2.29E+01
0.6	-2.29E+01
0.62	-2.29E+01
0.64	-2.28E+01
0.66	-2.28E+01
0.68	-2.28E+01
0.7	-2.27E+01
0.72	-2.27E+01
0.74	-2.26E+01
0.76	-2.25E+01
0.78	-2.24E+01
0.8	-2.23E+01
0.82	-2.21E+01

0.84	-2.19E+01
0.86	-2.17E+01
0.88	-2.13E+01
0.9	-2.08E+01
0.92	-2.00E+01
0.94	-1.88E+01
0.96	-1.70E+01
0.98	-1.42E+01
1	-9.98E+00
1.02	-3.88E+00
1.04	4.69E+00

Table 3 Analysis Varying Perovskite Thickness.

Table 3.a Cu₂O- Perovskite –SnO₂

Thickness	Open Circuit Voltage	Short Circuit Current	Fill Factor	Efficiency
μm	V _{oc} (V)	(mA/cm ²)	FF(%)	η (%)
0.2	0.9877	1.82E+01	74.34	13.39
0.30831	0.9796	2.12E+01	74.01	15.4
0.41662	0.9721	2.29E+01	74.08	16.49
0.52439	0.9657	2.38E+01	74.05	17.04
0.63324	0.9603	2.44E+01	73.84	17.27
0.74155	0.9552	2.46E+01	73.48	17.29
0.84986	0.9508	2.48E+01	72.95	17.18
0.95817	0.9469	2.48E+01	72.28	16.98
1.06648	0.9435	2.48E+01	71.48	16.72
1.17479	0.9403	2.47E+01	70.57	16.41
1.2831	0.9373	2.46E+01	69.59	16.07

1.39141	0.9345	2.45E+01	68.53	15.7
1.49972	0.9319	2.44E+01	67.4	15.32

Table 3.b Cu₂O -Perovskite-TiO₂

Thickness	Open Circuit Voltage	Short Circuit Current	Fill Factor	Efficiency
μm	V _{oc} (V)	(mA/cm ²)	FF(%)	η (%)
0.2	1.0198	1.82E+01	69.69	12.93
0.30831	1.0069	2.11E+01	70.45	14.98
0.41662	0.9917	2.27E+01	71.1	16.02
0.52439	0.9763	2.36E+01	71.33	16.46
0.63324	0.9618	2.42E+01	71.15	16.54
0.74155	0.949	2.44E+01	70.59	16.38
0.84986	0.9387	2.46E+01	69.68	16.08
0.95817	0.9307	2.46E+01	68.5	15.69
1.06648	0.9247	2.46E+01	67.14	15.26
1.17479	0.9201	2.45E+01	65.67	14.81
1.2831	0.9163	2.44E+01	64.17	14.35
1.39141	0.9132	2.43E+01	62.66	13.9
1.49972	0.9104	2.42E+01	61.19	13.46

Table 3.c Cu₂O –Perovskite- ZnO

Thickness	Open Circuit Voltage	Short Circuit Current	Fill Factor	Efficiency
μm	V _{oc} (V)	(mA/cm ²)	FF(%)	η (%)
0.2	1.0204	1.92E+01	71.15	13.94
0.30831	1.0125	2.15E+01	71.65	15.59
0.41662	1.0026	2.28E+01	70.85	16.21

0.52439	0.9917	2.36E+01	69.71	16.33
0.63324	0.9811	2.41E+01	68.48	16.19
0.74155	0.9703	2.44E+01	67.24	15.89
0.84986	0.96	2.45E+01	65.93	15.49
0.95817	0.9493	2.45E+01	64.66	15.05
1.06648	0.9391	2.45E+01	63.41	14.57
1.17479	0.9287	2.44E+01	62.22	14.1
1.2831	0.9191	2.43E+01	61.05	13.63
1.39141	0.9102	2.42E+01	59.9	13.18
1.49972	0.9032	2.40E+01	58.7	12.74

Table 3.d NiO_x –Perovskite-TiO₂

Thickness	Open Circuit Voltage	Short Circuit Current	Fill Factor	Efficiency
μm	V _{oc} (V)	(mA/cm ²)	FF(%)	η (%)
0.2	1.0421	1.89E+01	77.69	15.3
0.30831	1.0321	2.23E+01	76.13	17.55
0.41662	1.0173	2.44E+01	75	18.61
0.52439	1.001	2.56E+01	74	19
0.63324	0.9846	2.64E+01	72.99	19
0.74155	0.9692	2.69E+01	71.91	18.75
0.84986	0.9556	2.72E+01	70.69	18.37
0.95817	0.9445	2.73E+01	69.31	17.89
1.06648	0.926	2.74E+01	67.78	17.37
1.17479	0.9296	2.74E+01	66.15	16.83
1.2831	0.9248	2.73E+01	64.49	16.29
1.39141	0.921	2.72E+01	62.83	15.75
1.49972	0.9179	2.71E+01	61.23	15.24

Table 3.e NiO_x –Perovskite-SnO₂

Thickness	Open Circuit Voltage	Short Circuit Current	Fill Factor	Efficiency
μm	V _{oc} (V)	(mA/cm ²)	FF(%)	η (%)
0.2	1.0109	1.89E+01	79.8	15.24
0.30831	0.9988	2.23E+01	79.63	17.77
0.41662	0.9887	2.44E+01	78.9	19.03
0.52439	0.9804	2.57E+01	77.99	19.63
0.63324	0.9732	2.65E+01	77.01	19.84
0.74155	0.9672	2.70E+01	75.98	19.82
0.84986	0.962	2.73E+01	74.9	19.65
0.95817	0.9573	2.74E+01	73.78	19.38
1.06648	0.9532	2.75E+01	72.62	19.04
1.17479	0.9495	2.75E+01	71.41	18.66
1.2831	0.9462	2.75E+01	70.17	18.24
1.39141	0.9431	2.74E+01	68.89	17.81
1.49972	0.9403	2.73E+01	67.57	17.36

Table 3.f NiO_x-Perovskite-ZnO

Thickness	Open Circuit Voltage	Short Circuit Current	Fill Factor	Efficiency
μm	V _{oc} (V)	(mA/cm ²)	FF(%)	η (%)
0.2	1.037	2.02E+01	79.84	16.7
0.30831	1.0308	2.30E+01	78.78	18.66
0.41662	1.0203	2.47E+01	76.3	19.24
0.52439	1.0087	2.58E+01	73.41	19.11

0.63324	0.9972	2.65E+01	70.84	18.72
0.74155	0.986	2.69E+01	68.74	18.25
0.84986	0.975	2.72E+01	66.9	17.72
0.95817	0.9644	2.73E+01	65.21	17.16
1.06648	0.9539	2.73E+01	63.66	16.59
1.17479	0.9436	2.73E+01	62.21	16.02
1.2831	0.9333	2.72E+01	60.87	15.47
1.39141	0.9236	2.71E+01	59.61	14.94
1.49972	0.9148	2.70E+01	58.39	14.42

Table 4: Analysis Varying Perovskite Bulk Defect Density.

Table 4.a Cu₂O – Perovskite-TiO₂

Perovskite Defect Density	Open Circuit Voltage	Short Circuit Current	Fill Factor	Efficiency
$1/cm^3$	$V_{oc}(V)$	(mA/cm^2)	FF(%)	$\eta(\%)$
1.00E+13	1.0606	2.15E+01	80.26	18.26
3.33E+13	1.0606	2.15E+01	80.26	18.26
1.11E+14	1.0605	2.15E+01	80.23	18.25
3.68E+14	1.0604	2.15E+01	80.14	18.23
1.23E+15	1.0597	2.15E+01	79.84	18.15
4.08E+15	1.0575	2.15E+01	78.9	17.9
1.36E+16	1.0509	2.14E+01	76.28	17.19
4.52E+16	1.0324	2.14E+01	72.33	15.98
1.50E+17	0.9832	2.13E+01	70	14.65
5.00E+17	0.9012	2.09E+01	68.19	12.83

Table 4.b Cu₂O-Perovskite- SnO₂

Perovskite Defect Density	Open Circuit Voltage	Short Circuit Current	Fill Factor	Efficiency
$1/cm^3$	V _{oc} (V)	(mA/cm ²)	FF(%)	η(%)
1.00E+13	1.1783	2.16E+01	80.15	20.38
3.33E+13	1.1775	2.16E+01	80.02	20.33
1.11E+14	1.1749	2.16E+01	79.65	20.19
3.68E+14	1.1672	2.16E+01	78.79	19.84
1.23E+15	1.1462	2.16E+01	77.67	19.21
4.08E+15	1.1075	2.16E+01	76.94	18.39
1.36E+16	1.0611	2.16E+01	76.27	17.45
4.52E+16	1.0119	2.15E+01	75.24	16.39
1.50E+17	0.9614	2.14E+01	73.13	15.05
5.00E+17	0.909	2.10E+01	68.98	13.18

Table 4.c Cu₂O-Perovskite- ZnO

Perovskite Defect Density	Open Circuit Voltage	Short Circuit Current	Fill Factor	Efficiency
$1/cm^3$	V _{oc} (V)	(mA/cm ²)	FF(%)	η(%)
1.00E+13	1.0569	2.18E+01	77.74	17.92
3.33E+13	1.0568	2.18E+01	77.74	17.92
1.11E+14	1.0568	2.18E+01	77.74	17.91
3.68E+14	1.0565	2.18E+01	77.72	17.9
1.23E+15	1.0557	2.18E+01	77.66	17.88

4.08E+15	1.0532	2.18E+01	77.44	17.78
1.36E+16	1.0462	2.18E+01	76.73	17.49
4.52E+16	1.0298	2.17E+01	74.56	16.69
1.50E+17	0.9996	2.16E+01	69.62	15.03
5.00E+17	0.9479	2.11E+01	63.85	12.78

Table 4.d NiO_x-Perovskite-SnO₂

Perovskite Defect Density	Open Circuit Voltage	Short Circuit Current	Fill Factor	Efficiency
$1/cm^3$	V _{oc} (V)	(mA/cm ²)	FF(%)	η(%)
1.00E+13	1.1898	2.27E+01	88.28	23.86
3.33E+13	1.1892	2.27E+01	88.13	23.81
1.11E+14	1.1872	2.27E+01	87.69	23.65
3.68E+14	1.1809	2.27E+01	86.59	23.23
1.23E+15	1.1627	2.27E+01	84.93	22.43
4.08E+15	1.1265	2.27E+01	83.53	21.37
1.36E+16	1.0804	2.27E+01	82.32	20.2
4.52E+16	1.0311	2.27E+01	80.87	18.91
1.50E+17	0.9802	2.26E+01	78.72	17.41
5.00E+17	0.9277	2.22E+01	75.04	15.47

Table 4.e NiO_x-Perovskite-TiO₂

Perovskite Defect Density	Open Circuit Voltage	Short Circuit Current	Fill Factor	Efficiency
$1/cm^3$	V _{oc} (V)	(mA/cm ²)	FF(%)	η(%)
1.00E+13	1.0647	2.27E+01	87.24	21.1
3.33E+13	1.0647	2.27E+01	87.23	21.1
1.11E+14	1.0647	2.27E+01	87.21	21.1

3.68E+14	1.0646	2.27E+01	87.15	21.08
1.23E+15	1.0642	2.27E+01	86.96	21.02
4.08E+15	1.0631	2.27E+01	86.27	20.83
1.36E+16	1.0595	2.27E+01	84.19	20.25
4.52E+16	1.0482	2.27E+01	79.25	18.33
1.50E+17	1.0157	2.26E+01	74.75	17.13
5.00E+17	0.9321	2.22E+01	72.99	15.1

Table 4.f NiO_x-Perovskite-ZnO

Perovskite Defect Density	Open Circuit Voltage	Short Circuit Current	Fill Factor	Efficiency
$1/cm^3$	V _{oc} (V)	(mA/cm ²)	FF(%)	η(%)
1.00E+13	1.0625	2.33E+01	83.1	20.61
3.33E+13	1.0625	2.33E+01	83.1	20.61
1.11E+14	1.0624	2.33E+01	83.1	20.6
3.68E+14	1.0623	2.33E+01	83.09	20.6
1.23E+15	1.0618	2.33E+01	83.04	20.58
4.08E+15	1.0604	2.33E+01	82.9	20.51
1.36E+16	1.0558	2.33E+01	82.44	20.3
4.52E+16	1.0441	2.33E+01	80.92	19.67
1.50E+17	1.02	2.31E+01	76.71	18.11
5.00E+17	0.9778	2.27E+01	68.85	15.28

Table 5: Analysis Varying Perovskite-ETM Interface Defect Density.

Table 5.a Cu₂O-Perovskite-SnO₂

Interface Defect Density	Open Circuit Voltage	Short Circuit Current	Fill Factor	Efficiency	Defect Density of Perovskite

$1/cm^3$	$V_{oc}(V)$	(mA/cm^2)	FF(%)	$\eta(\%)$	$1/cm^3$
1E+13	1.1628	21.58	77.22	19.38	E15
1E+14	1.1511	21.58	77.84	19.33	E15
1E+15	1.1163	21.58	79.18	19.07	E15
1E+16	1.0679	21.57	79.62	18.34	E15
1E+17	1.0318	21.53	78.22	17.38	E15
1E+13	1.0736	21.57	76.45	17.70	E16
1E+14	1.0731	21.57	76.48	17.70	E16
1E+15	1.0688	21.57	76.69	17.68	E16
1E+16	1.0495	21.56	77.36	17.51	E16
1E+17	1.0236	21.52	76.94	16.95	E16
1E+13	0.9788	21.46	74.01	15.55	E17
1E+14	0.9787	21.46	74.01	15.55	E17
1E+15	0.9786	21.46	74.00	15.54	E17
1E+16	0.9776	21.46	73.91	15.51	E17
1E+17	0.9736	21.42	73.41	15.31	E17

Table 5.b Cu₂O – Perovskite-TiO₂

Interface Defect Density	Open Circuit Voltage	Short Circuit Current	Fill Factor	Efficiency	Defect Density of Perovskite
$1/cm^3$	$V_{oc}(V)$	(mA/cm^2)	FF(%)	$\eta(\%)$	$1/cm^3$
1E+13	1.118	2.15E+01	79.62	19.1	E15
1E+14	1.0599	2.15E+01	79.91	18.17	E15
1E+15	1.0004	2.15E+01	79.94	17.16	E15
1E+16	0.9449	2.14E+01	79.39	16.09	E15
1E+17	0.9077	2.14E+01	77.56	15.06	E15
1E+13	1.0937	2.14E+01	75.69	17.75	E16
1E+14	1.0532	2.14E+01	77.17	17.43	E16

1E+15	0.9983	2.14E+01	78.56	16.82	E16
1E+16	0.944	2.14E+01	78.83	15.95	E16
1E+17	0.9073	2.14E+01	77.29	14.99	E16
1E+13	1.0128	2.13E+01	70.03	15.13	E17
1E+14	1.0053	2.13E+01	70.53	15.13	E17
1E+15	0.977	2.13E+01	72.46	15.1	E17
1E+16	0.9343	2.13E+01	74.87	14.92	E17
1E+17	0.9026	2.13E+01	74.92	14.39	E17

Table 5.c Cu₂O – Perovskite-ZnO

Interface Defect Density	Open Circuit Voltage	Short Circuit Current	Fill Factor	Efficiency	Defect Density of Perovskite
$1/cm^3$	$V_{oc}(V)$	(mA/cm^2)	FF(%)	$\eta(\%)$	$1/cm^3$
1E+13	1.1205	21.804779	77.91	19.04	E15
1E+14	1.0559	21.804693	77.67	17.88	E15
1E+15	0.9931	21.803558	77.17	16.71	E15
1E+16	0.9359	21.783574	76.03	15.5	E15
1E+17	0.8977	21.601367	73.97	14.34	E15
1E+13	1.0924	21.791974	77.21	18.38	E16
1E+14	1.0487	21.791892	77	17.6	E16
1E+15	0.9908	21.790794	76.71	16.56	E16
1E+16	0.9348	21.771013	75.78	15.42	E16
1E+17	0.897	21.589398	73.82	14.3	E16
1E+13	1.0304	21.664636	70.68	15.78	E17
1E+14	1.0115	21.664595	71.6	15.69	E17
1E+15	0.9724	21.66386	72.94	15.37	E17
1E+16	0.9251	21.646092	73.52	14.72	E17

1E+17	0.8913	21.470351	72.39	13.85	E17
-------	--------	-----------	-------	-------	-----

Table 5.d NiO_x-Perovskite-SnO₂

Interface Defect Density	Open Circuit Voltage	Short Circuit Current	Fill Factor	Efficiency	Defect Density of Perovskite
$1/cm^3$	V _{oc} (V)	(mA/cm ²)	FF(%)	η(%)	$1/cm^3$
1E+13	1.1863	22.719756	84.23	22.7	E15
1E+14	1.167	22.719709	85.22	22.59	E15
1E+15	1.124	22.719246	86.47	22.08	E15
1E+16	1.0717	22.71474	86.42	21.04	E15
1E+17	1.0313	22.679619	84.95	19.87	E15
1E+13	1.0934	22.710592	82.59	20.51	E16
1E+14	1.0925	22.710545	82.64	20.5	E16
1E+15	1.0853	22.710083	83.03	20.47	E16
1E+16	1.0587	22.705588	84.04	20.2	E16
1E+17	1.0261	22.670551	83.79	19.49	E16
1E+13	0.9976	22.619387	79.56	17.95	E17
1E+14	0.9976	22.619342	79.56	17.95	E17
1E+15	0.9974	22.618891	79.57	17.95	E17
1E+16	0.9955	22.614503	79.58	17.92	E17
1E+17	0.9886	22.580284	79.44	17.73	E17

Table 5.e NiO_x-Perovskite-TiO₂

Interface Defect Density	Open Circuit Voltage	Short Circuit Current	Fill Factor	Efficiency	Defect Density of Perovskite
$1/cm^3$	V _{oc} (V)	(mA/cm ²)	FF(%)	η(%)	$1/cm^3$

1E+13	1.1253	2.27E+01	87.24	22.3	E15
1E+14	1.0643	2.27E+01	87	21.04	E15
1E+15	1.004	2.27E+01	86.43	19.71	E15
1E+16	0.9471	2.27E+01	85.43	18.38	E15
1E+17	0.9061	2.27E+01	83.6	17.17	E15
1E+13	1.1093	2.27E+01	84.08	21.18	E16
1E+14	1.0608	2.27E+01	84.96	20.46	E16
1E+15	1.0028	2.27E+01	85.36	19.44	E16
1E+16	0.9466	2.27E+01	84.98	18.26	E16
1E+17	0.9058	2.27E+01	83.39	17.12	E16
1E+13	1.0462	2.26E+01	74.89	17.72	E17
1E+14	1.0306	22.619436	75.99	17.71	E17
1E+15	0.9904	2.26E+01	78.79	17.65	E17
1E+16	0.9406	2.26E+01	81.39	17.31	E17
1E+17	0.9028	2.26E+01	81.43	16.59	E17

Table 5.f NiO_x-Perovskite-ZnO

Interface Defect Density	Open Circuit Voltage	Short Circuit Current	Fill Factor	Efficiency	Defect Density of Perovskite
$1/cm^3$	V _{oc} (V)	(mA/cm ²)	FF(%)	η(%)	$1/cm^3$
1E+13	1.1305	23.335985	83.75	22.1	E15
1E+14	1.062	23.335272	83.06	20.58	E15
1E+15	0.9979	23.328929	81.97	19.08	E15
1E+16	0.9388	23.287239	80.47	17.59	E15
1E+17	0.8963	23.07723	78.56	16.25	E15

1E+13	1.109	23.324169	83.48	21.59	E16
1E+14	1.0575	23.323464	82.61	20.38	E16
1E+15	0.9964	23.317185	81.65	18.97	E16
1E+16	0.9381	23.275756	80.28	17.53	E16
1E+17	0.8959	23.06632	78.44	16.28	E16
1E+13	1.0545	23.206574	78.09	19.11	E17
1E+14	1.0298	23.205947	78.56	18.77	E17
1E+15	0.984	23.200299	78.83	18	E17
1E+16	0.9314	23.161465	78.51	16.94	E17
1E+17	0.8921	22.957716	77.29	15.83	E17

References

1. <http://whatis.techtarget.com/definition/renewable-energy>; FEBRUARY 2018 AT 12:31:20PM
2. HTTPS://WWW.SCIENCEDAILY.COM/TERMS/RENEWABLE_ENERGY.HTM; FEBRUARY 2018 AT 12:31:20PM
3. <HTTP://WWW.ALTERNATIVE-ENERGY-TUTORIALS.COM/ENERGY-ARTICLES/RENEWABLE-ENERGY-SOURCES-A-BRIEF-SUMMARY.HTML>; FEBRUARY 2018 AT 12:31:20PM
4. https://www.google.com/search?q=ren21+2017&source=lnms&tbm=isch&sa=X&ved=0ahUKEwiC2rGOl_HZAhUKqo8KH7KDIIQ_AUICygC&biw=1350&bih=610#imgrc=AI65sCom0Z9DhM; FEBRUARY 2018 at 9:45:20pm [5]
5. <https://www.energy.gov/eere/solar/crystalline-silicon-photovoltaics-research>; 8th march.2018; 11:30:20 am.
6. Martin A. Green, 'Solar cell efficiency tables (Version 45)', progress in photovoltaics, Volume 23, Issue 1, Pages 1–9,2015
7. Martin A. Green, 'Solar cell efficiency tables (Version 45)', progress in photovoltaics, Volume 23, Issue 1, Pages 1–9,2015
8. https://www.iapp.de/iapp/agruppen/osol/?Research:Organic_Solar_Cells:Basics_of_OSC; June 30.2017, 12:24:20pm
9. Martin A. Green, 'Solar cell efficiency tables (Version 45)', progress in photovoltaics, Volume 23, Issue 1, Pages 1–9,2015
10. Martin A. Green, 'Solar cell efficiency tables (Version 45)', progress in photovoltaics, Volume 23, Issue 1, Pages 1–9,2015
11. Hoppe, Harald & Serdar Sariciftci, N. (2007). Polymer Solar Cells. Advances in Polymer Science. 214. 1-86. 10.1007/12_2007_121.
12. Anthony N. Stranges, 'Solar energy', journal of chemical energy, vol-61,3, march 1984
13. <https://warstek.com/2018/01/08/psc-2/>; last access: 0:57,28th February 2018
14. (SCAPS)
36. (Cu₂O)

37. D. S. GINLEY AND ET AL, HANDBOOK OF TRANSPARENT CONDUCTORS. NEW YORK:
SPRINGER, 2010.